Computers and Structures 112–113 (2012) 364–379

Contents lists available at SciVerse ScienceDirect

Computers and Structures

journal homepage: www.elsevier.com/locate/compstruc

# Combined parametric–nonparametric uncertainty quantification using random matrix theory and polynomial chaos expansion

B. Pascual, S. Adhikari *

*College of Engineering, Swansea University, Singleton Park, Swansea SA2 8PP, United Kingdom*

ARTICLE INFO

*Article history:*
Received 26 January 2012
Accepted 27 August 2012
Available online 6 October 2012

*Keywords:*
Stochastic systems
Uncertainty propagation
Polynomial chaos
Wishart matrix

ABSTRACT

Propagation of combined parametric and nonparametric uncertainties in elliptic partial differential equations is considered. Two cases, namely, (a) both uncertainties are over the entire domain, and (b) different types of uncertainties are over non-overlapping subdomains are proposed. Parametric uncertainty is modelled by a random field and is discretised using the Karhunen–Loève (KL) expansion. The nonparametric uncertainty is modelled by Wishart random matrix. Both uncertainties are considered independent, and the two first moments of the response are calculated using polynomial chaos expansion and analytical random matrix theory results. Closed-form analytical expressions of the first two moments are derived for both cases.



## 1. Introduction

Uncertainty quantification in structures has been a popular topic for the last five decades, due to its influence on subjects such as structures reliability and model validation amongst others. The first kind of uncertainties studied were the uncertainties introduced by random forces applied to the structure [1]. Then followed the study of the case where uncertainty is introduced by random variables or by random fields modeling material properties (e.g., Young's modulus, mass density, Poisson's ratio, damping coefficient) or geometric parameters. This topic has been researched extensively over the last three decades. A third kind of uncertainty, known as epistemic/model uncertainty has been introduced during the last decade. This kind of uncertainty does not explicitly depend on the system parameters, but models the system matrices as multivariate distributions. The method is aimed at, for example, unquantified errors associated with the equation of motion, the damping model or the model of structural joints. The method is also used for errors associated with the numerical methods, as discretization of displacement fields, truncation and roundoff errors, tolerances in the optimization and iterative algorithms or step-sizes in the time-integration methods. The system considered is modelled with a linear partial differential equation (e.g., stationary elliptic PDE) and this equation can be discretized with the finite element method (FEM) (e.g., [2]). Then, for a system with $n$ number of degrees of freedom, a vector of nodal response $\mathbf{u} \in \mathbb{R}^n$, a linear operator or stiffness matrix $\mathbf{K} \in \mathbb{R}^{n\times n}$ and a forcing term $\mathbf{f} \in \mathbb{R}^n$ are related through the equation

$$\mathbf{K}\mathbf{u} = \mathbf{f} \tag{1}$$

The uncertainty appearing as random forces applied to the structure is included in the random forcing term $\mathbf{f}$. For data/aleatoric uncertainties, statistics of the system parameters (Young's modulus, etc.) can be described through their joint probability density function (pdf) or as functions of known random variables. Then, the uncertainty of the parameters is propagated to the stiffness matrix, that becomes a random matrix as a consequence. Both parametric (aleatoric) and nonparametric (epistemic) uncertainties in system Eq. (1) can be completely characterized by the joint pdf of $\mathbf{K}$ and $\mathbf{f}$. The method for obtaining this joint pdf will depend on the nature of uncertainties.

If aleatoric uncertainty is considered and parameters are modeled using random fields, the stochastic finite element method (SFEM) can be used to obtain the response of the system. The first step of the method consists in discretizing the random field (see, for example [3–5]) so as to obtain a linear operator $\mathbf{K}$ depending on a set of uncorrelated random variables. Then the response of the system can be approximated by several methods [4,6,7]. The most widely used SFEMs include simulation-based methods (e.g., Monte Carlo Simulation (MCS) [8], collocation method [9,10]), expansion-based methods (perturbation method [11], Neumann expansion method [12], spectral approach [13,14,6,7]), expansion approaches combined with system reduction methods [15–18] and algebraic approaches [19,20].

Quantification of nonparametric uncertainties, unlike parametric uncertainty, is not suited to usual parameter estimation techniques. Methods to evaluate this type of uncertainties in the

* Corresponding author. Tel.: +44 (0) 1792 602088; fax: +44 (0) 1792 295676.
*E-mail address:* s.adhikari@swansea.ac.uk (S. Adhikari).
*URL:* http://engweb.swan.ac.uk/~adhikaris/ (S. Adhikari).

0045-7949/$ - see front matter © 2012 Elsevier Ltd. All rights reserved.
http://dx.doi.org/10.1016/j.compstruc.2012.08.008

context of multiple-degrees-of-freedom systems can be based on random matrix theory (RMT) [21]. The matrix variate distributions used are obtained using the maximum entropy principle [22] for positive symmetric real random matrices [23,24]. The resulting random matrix can be called Wishart matrix or matrix variate gamma distribution, as both probability density functions coincide under some conditions [21,25]. A Wishart matrix distribution $W_n(p,\mathbf{\Sigma})$ is completely characterized by its parameters $p$ and $\mathbf{\Sigma} \in \mathbb{R}^{n\times n}$. The parameters of the Wishart matrix variate distribution can be related to the mean of the distribution and to a measure of uncertainty, the dispersion parameter [24]. Different criterion were proposed by Adhikari [26] to fit the parameters arising in the Wishart distribution. Recently, Ghanem and Das [27] coupled frequency response function matrices with Wishart random matrices.

It can be observed that methods to deal with parametric and nonparametric uncertainties have been developed independently. However, both kinds of uncertainties can affect real-life structures simultaneously. In many cases, both uncertainties can affect the same domain of a complex system. As an example, the case of a flow through porous media problem, where permeability is modeled with a random field, but the mapping of this random field into the system operator is not completely known. Another example can be a complex structure such as an aircraft where liner elasticity model with uncertain parameter is used. At the same time there are model uncertainties arising from the lack of precise modelling of the structural joints. Therefore, there is a need to model both parametric and nonparametric uncertainties simultaneously within the same domain of a system. A different case may arise for structures composed of several components such a fuselage, wing and engines of an aircraft. Here the parametric uncertainties affecting some parts can be known, however the modeling of the other parts can be subjected to errors or simplifications. Here also both kinds of uncertainties, in different domains of a same system, should be considered simultaneously. In this paper we propose approaches to model parametric and nonparametric uncertainties for these two different possible cases. Based on this combined uncertainty modelling, new analytical methods are developed for efficient propagation of such uncertainties through finite element models. The first type of combined uncertainty considers that both parametric and nonparametric uncertainty affect the whole domain of the system, while the second type of combined uncertainty considers that each type of uncertainty affects a different subdomain of the system. The first and second moments of the response are obtained by combining results from Polynomial Chaos to deal with parametric uncertainty and from analytical expressions of moments of the inverted Wishart matrix to deal with nonparametric uncertainty.

The outline of the paper is as follows. The basics of parametric and nonparametric uncertainty are recalled in Sections 2 and 3. The case where both kinds of uncertainties appear on overlapped domains is dealt with in Section 4. The case of different uncertainties appearing over non-overlapping domains is considered in Section 5. Two methods are proposed based on substructuring techniques to obtain mean and standard deviation of the response. Each method uses a different technique to ensure positive definiteness of the system operator. The proposed combined approaches are applied to an Euler–Bernoulli beam problem and a flow through porous media problem.

## 2. Parametric uncertainty

Parametric uncertainty can be introduced in the system by parameters such as Young's modulus and Poisson's ratio amongst others. When uncertainty in the system is parametric, it can be described using probability theory and modelled by a random field [3–5], defined on a probability space $(\Omega,\mathcal{F},P)$ where $\Omega$ is the sample space, $\mathcal{F}$ is the $\sigma$-algebra of events and $P$ is the probability measure. In the probability space, a random variable $X$ is a function whose domain is $\Omega$, $X:(\Omega,\mathcal{F},P)\to\mathbb{R}$, inducing a probability measure on $\mathbb{R}$ called the probability distribution of $X$, $P_X$. A random field $H(x,\omega)$ is a collection of random variables indexed by $x$ related to the system geometry. Parameters are implemented in the system model through discretization of the random fields used to model them, that is, it is assumed that uncertainty can be represented by a finite set of random variables defining a new probability space $(\Xi,\mathcal{F}_\Xi,P_\Xi)$. If a random field has finite variance, it can be projected on a basis of functions of the Hilbert space denoted by $\mathcal{L}^2(\Xi,dP_\Xi)$, a property that can be used when discretizing a random field.

There are three groups of discretization schemes, namely, point discretization, average discretization and series expansion. More details are given in [28,4,5]. Here we focus on two types of series expansion methods, the Karhunen–Loève (KL) expansion and polynomial chaos (PC) expansion. Both methods expand any realization of the original random field over a complete set of deterministic functions and truncates the series after a finite number of terms.

### 2.1. Random field discretization with Karhunen–Loève expansion

The Karhunen–Loève (KL) expansion expands the random field with a Fourier-type series and is based on the spectral decomposition of the autocorrelation function. The KL expansion of a random field $H(x)$ is given by

$$H(x) = \mathrm{E}[H(x)] + \sum_{i=1}^{\infty}\sqrt{\lambda_i}\xi_i\varphi_i(x) \tag{2}$$

with $\mathrm{E}[H(x)]$ the mean of the random field, $f_n(x)$ a set of orthonormal functions (i.e., $\int_{\mathcal{D}}\varphi_n(x)\varphi_m^*(x)dx=\delta[n-m]$) and $(\xi_1,\ldots,\xi_n)$ a set of uncorrelated random variables (i.e., $E[\xi_n\xi_m]=\delta_{nm}$). The constants $\lambda_n$ and functions $\varphi_n(x)$ are the eigenvalues and eigenfunctions of the autocorrelation function $\mathrm{R}(x_1,x_2)$ of $H(x)$. That is, $\lambda_n$ and $\varphi_n(x)$ are obtained from the equation

$$\int_{\mathcal{D}}\mathrm{R}(x_1,x_2)\varphi(x_2)dx_2 = \lambda\varphi(x_1) \tag{3}$$

where $\mathcal{D}$ is the domain where the autocorrelation function is defined. A homogeneous Gaussian random field with exponential autocorrelation function is considered, that is, $\mathrm{R}(x_1,x_2)=e^{-|x_1-x_2|/b}$, where $b$ is the correlation length. For this case, explicit solution for the eigenvalues and eigenvectors are available [13] and the KL expansion of the random field is obtained by introducing these solutions into Eq. (2). The parametric uncertainty is then propagated to the system matrices arising in the Finite Element method by taking into account the effect of the eigensolution on the element matrices. When considering the case of a stationary linear partial differential equation (PDE), the equation can be discretized using the Finite Element method to obtain a linear algebraic equation $\mathbf{Ku}=\mathbf{f}$ [2]. When a parameter of the system is represented by a random field, the random field can be discretized using its KL expansion. The algebraic equation resulting from the propagation of the random field into the system matrix can be given by

$$\left(\mathbf{K}_0+\sum_{i=1}^{M}\mathbf{K}_i\xi_i\right)\mathbf{u}=\mathbf{f} \tag{4}$$

where the KL expansion has been truncated after $M$ terms. The element stiffness matrices given by

$$\mathbf{K}_0^e = \int_{\Omega_e}\mathbf{B}^{(e)\,T}(x)\mathbf{D}\mathbf{B}^{(e)}(x)\,dx \tag{5}$$

$$\mathbf{K}_i^e = \sqrt{\lambda_i}\int_{\Omega_e}\varphi_i(x)\mathbf{B}^{(e)\,T}(x)\mathbf{D}\mathbf{B}^{(e)}(x)\,dx \tag{6}$$

$\mathbf{B}^{(e)}$ is the matrix relating the strain components to nodal displacements, $\mathbf{D}$ is the constitutive matrix, $\mathbf{u}$ is the response vector and $\mathbf{f}$ is the forcing term. For a 1D problem $\mathbf{B}^{(e)} = d\mathbf{N}^{(e)}/dx$, with $\mathbf{N}^{(e)}$ the matrix of shape functions.

### 2.2. Polynomial chaos approach to the stochastic finite element method

The Stochastic Finite Element Method (SFEM) consists in solving Eq. (4) and several methods have been proposed, amongst them Polynomial Chaos. Polynomial Chaos expansion allows to project a second-order random variable $X$ into the Hilbert space $\mathcal{L}^2(\Xi, dP_\Xi)$. Consequently, a series expansion $X = \sum_{i=1}^{\infty} c_i \Gamma_i(\omega)$ is obtained, where $c_i$ are unknown constants and $\Gamma_i(\xi_1,\ldots,\xi_m)$ are a set of basis functions of the Hilbert space. The series is truncated after $P$ terms. Their first applications in SFEM used Hermite polynomial chaos as basis functions [13], but other basis have been used, as the Wiener–Askey polynomial chaos [29], wavelets [30], multi-element method [31–33], finite elements [14], Padé–Legendre approximants [34] or an orthogonal polynomial basis generated by a nonstandard pdf [35,32]. In this paper, the Polynomial Chaos method is used, where the basis functions are derived from univariate Hermite polynomials. The univariate Hermite polynomial of order $q$ is obtained from

$$H_q(\xi) = (-1)^q \exp(\xi^2/2)\frac{\partial^q \exp(-\xi^2/2)}{\partial^q \xi} \tag{7}$$

and each set of univariate Hermite polynomials depend on a different random variable $\xi_j$. The basis functions $\Gamma_i$ are obtained from the terms of the tensor product of several univariate Hermite polynomials up to a fixed total-order specification $p$, this approach is referred to as "total-order expansion", and the number of polynomials obtained is $P = (m+p)!/m!p!$.

In Eq. (4), the response vector and forcing term can be expanded with the PC expansions

$$\mathbf{u}^{(\mathrm{PC})} = \sum_{i=1}^{P} \mathbf{u}_i \Gamma_i \tag{8}$$

$$\mathbf{f}^{(\mathrm{PC})} = \sum_{i=1}^{P} \mathbf{f}_i \Gamma_i \quad \text{with} \quad \mathbf{f}_i = \frac{\mathrm{E}[\mathbf{f}\Gamma_i]}{\mathrm{E}\left[\Gamma_i^2\right]} \tag{9}$$

Two approaches stand out in the literature to calculate the vectors of coefficients $\mathbf{u}_i$ of the PC expansions, namely, Galerkin methods and non-intrusive methods [7]. In Galerkin methods, the vectors of coefficients $\mathbf{u}_i$ of the PC expansions can be retrieved by ensuring that the residual of Eq. (4) is orthogonal to each basis $\Gamma_i$. Mathematically, this condition is achieved by multiplying Eq. (4) by each basis function $\Gamma_p$, $p = 1,\ldots,P$ and taking the mean of the resulting equation

$$\sum_{i=1}^{P}\left(\mathbf{K}_0 \mathrm{E}[\Gamma_i\Gamma_p] + \sum_{i=1}^{M}\mathbf{K}_i \mathrm{E}[\xi_i\Gamma_i\Gamma_p]\right)\mathbf{u}_i = \mathbf{f}_p \mathrm{E}\left[\Gamma_p^2\right] \tag{10}$$

A linear deterministic equation of size $n \times P$ is obtained

$$\mathbf{A}^{(\mathrm{PC})}\mathbf{u}_{\mathbf{c}} = \mathbf{f}_{\mathbf{c}}, \qquad \mathbf{A}^{(\mathrm{PC})} = \left(\mathbf{d}\otimes\mathbf{K}_0 + \sum_{i=1}^{M}\mathbf{c}_i\otimes\mathbf{K}_i\right) \tag{11}$$

where $\otimes$ is the kronecker product. The vector of coefficients and the forcing vector are given respectively by $\mathbf{u}_{\mathbf{c}} = \left[\mathbf{u}_1^T, \mathbf{u}_2^T, \ldots, \mathbf{u}_P^T\right]^T$ and $\mathbf{f}_{\mathbf{c}} = [\mathrm{E}[\mathbf{f}\Gamma_1]^T,\ldots,\mathrm{E}[\mathbf{f}\Gamma_P]^T]^T$. The diagonal matrix $\mathbf{d}$ with diagonal entries $\mathbf{d}_{ii} = \mathrm{E}\left[\Gamma_i^2\right]$ and matrices $\mathbf{c}_i$ whose elements are given by $\mathbf{c}_{i_{jk}} = \mathrm{E}[\xi_i\Gamma_j\Gamma_k]$ depend on the Polynomial Chaoses used as basis functions, and are therefore problem-independent. It is noted that for a deterministic forcing term $\mathbf{f}_i = 0$ for $i > 1$ and $\mathbf{f}_1 = \mathbf{f}$, so that $\mathbf{f}_{\mathbf{c}} = [\mathbf{f}^T, 0, \ldots, 0]^T$.

The non-intrusive methods are based on calculating the vectors of coefficients $\mathbf{u}_i$ through numerical integration [36] by noting that

$$\mathbf{u}_i = \frac{\mathrm{E}[\Gamma_i\mathbf{u}]}{\mathrm{E}\left[\Gamma_i^2\right]} \tag{12}$$

The integral $\mathrm{E}\left[\Gamma_i^2\right]$ can be obtained analytically, as it is one of the diagonal entries of $\mathbf{d}$, and only $\mathrm{E}[\Gamma_i\mathbf{u}]$ remains to be calculated. For a system with one random variable $\xi_j$, this integral can be calculated through a quadrature method, that is, $\mathrm{E}[\Gamma_i\mathbf{u}] \approx \sum_{k=1}^{p+1}\Gamma_i(\xi_{j_k})\mathbf{u}(\xi_{j_k})A_k$, where $\xi_{jk}$ are the roots of an orthogonal polynomial with respect to a weight function $W(\xi)$ and $A_k$ are the corresponding weights. This numerical quadrature allows to integrate exactly polynomials up to order $2p+1$ with respect to a weight function. If Hermite polynomials from Eq. (7) are used, the weight function can be $W(\xi) = e^{-\xi^2/2}/2\pi$. For a system with $M$ random variables, the integral is approximated through a cubature method [37], that can be a tensor product or a sparse grid method based on a quadrature method. For the case of a tensor product combined with Gauss–Hermite quadrature, the solution of Eq. (4) is calculated for the combinations of random variables $\xi_1,\ldots,\xi_M$ where each random variable $\xi_j$ takes the values of the zeros of the Hermite polynomial of order $p+1$, and there are $(p+1)^M$ combinations. A combination of values adopted by the random variables is denoted by $\xi_{1j_1},\ldots,\xi_{Mj_M}$, so that $\xi_{kj_k}$ is a zero of the Hermite polynomial. The tensor product approximation to the integral using quadrature formula is given by

$$\mathrm{E}[\Gamma_i\mathbf{u}] \approx \sum_{j=1}^{(p+1)^M}\left(\Gamma_i(\xi_{1j_1},\ldots,\xi_{Mj_M})\mathbf{u}(\xi_{1j_1},\ldots,\xi_{Mj_M})\prod_{k=1}^{M}A_{j_k}\right) \tag{13}$$

with each weight of the quadrature formula given by [38]

$$A_{j_k} = \int_{-\infty}^{+\infty}\frac{e^{-\xi_k^2/2}}{2\pi}\left(\prod_{l\neq k,l=1}^{p+1}\frac{\xi_k-\xi_{kj_l}}{\xi_{kj_k}-\xi_{kj_l}}\right)^2 d\xi_k \tag{14}$$

The weights can be calculated exactly, noting that the moments of a normal random variable are such that $\mathrm{E}[\xi^n] = \int_{-\infty}^{+\infty}\xi^n e^{-\xi^2/2}/2\pi d\xi = 1.3\ldots(n-1)$ for $n$ even and 0 for $n$ odd. For a cubature method based on sparse grid, the solution is calculated at a smaller number of nodes [37]. After obtaining the PC expansion of the response, the first and second moments of the response can be retrieved

$$\mathrm{E}[\mathbf{u}] = \sum_{i=1}^{P}\mathbf{u}_i\mathrm{E}[\Gamma_i] = \mathbf{u}_1 \tag{15}$$

$$\mathrm{E}[\mathbf{u}\mathbf{u}^T] = \sum_{i,j=1}^{P}\mathbf{u}_i\mathbf{u}_j^T\mathrm{E}[\Gamma_i\Gamma_j] = \sum_{i=1}^{P}\mathbf{u}_i\mathbf{u}_i^T\mathrm{E}\left[\Gamma_i^2\right] \tag{16}$$

and the standard deviation of the $i$-th element of vector $\mathbf{u}$, i.e., $u_i$, is given by

$$\sigma_{u_i}^2 = \sqrt{\mathrm{E}\left[u_i^2\right] - \mathrm{E}[u_i]^2} \tag{17}$$

where $\mathrm{E}\left[u_i^2\right]$ is the $i$-th diagonal element of the matrix $\mathrm{E}[\mathbf{u}\mathbf{u}^T]$.

## 3. Nonparametric uncertainty

Characterizing parametric uncertainty follows several steps, namely, identification of the random parameters, probabilistic description of these parameters and mapping of the parameters into the system matrices. To quantify uncertainty in a system while avoiding the difficulties that are inherent to the steps followed to characterize parametric uncertainty, Soize [24,39] proposed a method that models system matrices as a random matrix. The approach is based on the information available on the system, i.e., matrices are symmetric positive definite second-order random variables as are their inverses. Then, the maximum entropy

method is used to obtain a joint pdf of the elements of the random matrix. The obtained distribution has the pdf corresponding to the Wishart distribution [25,21], under some conditions [26].

### 3.1. Wishart distribution

Let us consider a symmetric positive definite matrix $\mathbf{G} \in \mathbb{R}^{n\times n}$. This matrix can be given by $\mathbf{G} = \mathbf{Z}^T\mathbf{Z}$, with $\mathbf{Z}$ a rectangular matrix of dimensions $p \times n$ with $p > n$. Consider that the $p \times n$ matrix $\mathbf{Z}$ is given by $N(\mathbf{0}_{p\times n}, \mathbf{I}_p \otimes \mathbf{\Sigma})$. That is, the $p$ rows of $\mathbf{Z}$ are independent $N_n(\mathbf{0}_{1\times n}, \mathbf{\Sigma})$ random vectors, and $\mathbf{0}_{n\times p}$ is a matrix $\in \mathbb{R}^{n\times p}$ whose elements are all equal to zero. Then, the distribution of $\mathbf{G} = \mathbf{Z}^T\mathbf{Z}$ is called a Wishart distribution [25,21]. A Wishart distribution is a $n$-variate generalization of $\chi^2$ distribution denoted by $W_n(p,\mathbf{\Sigma})$ with parameters $p$,$n$ and $\mathbf{\Sigma}(n \times n) > 0$, has dimension $n \times n$, is symmetric positive definite and its probability density function is given by [25,21]

$$p_{\mathbf{G}} = \left\{2^{\frac{1}{2}np}\Gamma_n\left(\frac{1}{2}p\right)\det(\mathbf{\Sigma})^{\frac{1}{2}p}\right\}^{-1}\det(\mathbf{G})^{\frac{1}{2}(p-n-1)} \exp\left\{\mathrm{Trace}\left(-\frac{1}{2}\mathbf{\Sigma}^{-1}\mathbf{G}\right)\right\}, \mathbf{G} > 0, p \geqslant n \tag{18}$$

where $\Gamma_n$ is the multivariate gamma function. This pdf can be obtained as the pdf maximizing the entropy $\mathcal{S}$ associated with the matrix variate probability density function $p_{\mathbf{G}}(\mathbf{G})$ [26]

$$\mathcal{S}(p_{\mathbf{G}}) = -\int_{\mathbf{G}>0} p_{\mathbf{G}}(\mathbf{G})\ln\{p_{\mathbf{G}}(\mathbf{G})\}\,d\mathbf{G} \tag{19}$$

The entropy equation is subjected to several constraints, that is, the matrix $\mathbf{G}$ is symmetric, nonnegative definite and

$$\int_{\mathbf{G}>0} p_{\mathbf{G}}(\mathbf{G})\,d\mathbf{G} = 1 \tag{20}$$

$$\mathrm{E}[\mathbf{G}] = \int_{\mathbf{G}>0} \mathbf{G}\,p_{\mathbf{G}}(\mathbf{G})\,d\mathbf{G} = \mathbf{G}_0 \tag{21}$$

$$\mathrm{E}[\ln\{\det(\mathbf{G})\}] = \nu, \quad |\nu| < +\infty \tag{22}$$

where $\mathbf{G}_0$ is the mean of matrix $\mathbf{G}$ and is prescribed. In general, the probability density function resulting from this analysis is a matrix variate gamma distribution. The main difference between the matrix variate gamma distribution and the Wishart distribution is that historically only integer values were considered for the parameter $p$ in the Wishart matrices. Then, the pdf $p_{\mathbf{G}}$ from Eq. (18) is called in this paper Wishart distribution probability density function and the parameters of the distribution are $p$ and $\mathbf{\Sigma} = \mathbf{G}_0/p$, that is $\mathbf{G} \sim W_n(p, \mathbf{G}_0/p)$.

### 3.2. Parameter selection

As already exposed, in nonparametric uncertainty the positive definite matrix that is assumed random is modeled by a Wishart matrix, and this matrix can be the system matrix or a submatrix of the global matrix. To model the matrix, it is assumed that the mean of this random matrix coincides with the deterministic matrix. This allows to determine matrix $\mathbf{\Sigma}$, but parameter $p$ remains to be calculated. The dispersion parameter $\delta_G$, a measure of the normalized standard deviation, was introduced by Soize [24]

$$\delta_G^2 = \frac{\mathrm{E}\left[\|\mathbf{G} - \mathrm{E}[\mathbf{G}]\|_{\mathrm{F}}^2\right]}{\|\mathrm{E}[\mathbf{G}]\|_{\mathrm{F}}^2}. \tag{23}$$

For a Wishart distribution it has been shown that [26]

$$\delta_G^2 = \frac{1}{p}\left\{1 + \frac{\{\mathrm{Trace}(\mathbf{G}_0)\}^2}{\mathrm{Trace}\left(\mathbf{G}_0^2\right)}\right\} \tag{24}$$

When underlying parametric uncertainty is considered and no experimental data are available, the dispersion parameter can be considered as a parameter to perform a sensitivity analysis of the stochastic solution. If experimental data are available, the dispersion parameter can be estimated through Eq. (23). The parameter $p$ of the Wishart distribution can be related to the dispersion parameter through Eq. (24), leading to

$$p = \frac{1}{\delta_G^2}\left\{1 + \frac{\{\mathrm{Trace}(\mathbf{G}_0)\}^2}{\mathrm{Trace}\left(\mathbf{G}_0^2\right)}\right\}. \tag{25}$$

Therefore, the parameter $p$ of the Wishart distribution can be calculated from the dispersion parameter and the mean of the matrix under consideration. It is noted here that other methods to fit the mean matrix have been proposed [26,40], where several criteria were selected. These criteria include the one adopted here where the mean of the stiffness matrix coincides with the mean of the random matrix. A second criterion stated that the mean of the inverse Wishart matrix coincides with the inverse of the mean stiffness matrix. The third criterion satisfied that the mean of the random matrix and the mean of the inverse of the random matrix are closest to the deterministic matrix and its inverse.

### 3.3. Simulation of Wishart matrices

In an algebraic linear system, a positive definite matrix $\mathbf{G}$ can be approximated with a Wishart matrix following the nonparametric approach. A Monte Carlo Simulation of the resulting Wishart distribution can be performed to obtain quantities of interest (e.g., moments of the response $\mathbf{u}$). The steps to perform the MCS simulation are [26].

1. Find the mean system matrix $\mathbf{G}_0$, that is, the matrix obtained from the deterministic FEM, and its dimension $n$. For complex engineering systems $n$ can be in the order of several thousands or even millions.
2. Obtain the normalized standard deviations or the 'dispersion parameters' $\tilde{\delta}_G \equiv \{\tilde{\delta}_G\}$ corresponding to the system matrix, from experiment, experience or using the Stochastic FEM.
3. Calculate

$$p = \frac{1}{\delta_G^2}\left\{1 + \frac{\{\mathrm{Trace}(\mathbf{G}_0)\}^2}{\mathrm{Trace}\left(\mathbf{G}_0^2\right)}\right\}. \tag{26}$$

and approximate it to its nearest integer. This approximation would introduce negligible error. Calculate $\mathbf{\Sigma} = \mathbf{G}_0/p$.

4. Create a $p \times n$ matrix $\widetilde{\mathbf{X}}$ with Gaussian random numbers with zero mean and unit covariance i.e., $\widetilde{\mathbf{X}} \sim N_{p,n}(\mathbf{O}, \mathbf{I}_p \otimes \mathbf{I}_n)$. Obtain the Cholesky decomposition of the positive definite matrix $\mathbf{\Sigma}$, $\mathbf{\Sigma} = \mathbf{\Gamma}\mathbf{\Gamma}^T$ and use it to calculate the matrix $\mathbf{Z}$ using the linear transformation

$$\mathbf{Z} = \widetilde{\mathbf{X}}\mathbf{\Gamma}^T \tag{27}$$

Obtain the sample of the Wishart matrix $\mathbf{G} = \mathbf{Z}^T\mathbf{Z}$.

5. Solve the equilibrium equation for each sample to obtain the response statistics of interest.

If one implements this approach in conjunction with a commercial finite element software, the commercial software needs to be accessed only once to obtain the mean matrices. This simulation procedure is therefore non-intrusive in nature.

## 4. Combined uncertainty over the entire domain

### 4.1. Problem description

Combined uncertainty over the same domain arises, for example, in flow through porous media, where the permeability can be described by a random field but at the same time the model used is not completely well known. This kind of uncertainty arises, more generally, when parametric uncertainties and uncertainties induced by modelling errors can be separated. Random matrix model is derived via the maximum entropy principle. It needs the information of the mean matrices to construct the random matrix model. This mean matrix itself may be imprecisely known in many cases. This mean matrix is what we model using random variables. That is, there are cases where the mean model of the nonparametric uncertainty can be affected by parametric uncertainty. Both parametric and nonparametric uncertainties have been considered by Soize [41] for dynamic systems. The effect of the two kinds of uncertainties has been compared in [42]. In Fig. 1 a domain affected by both parametric and nonparametric uncertainty is considered, where parametric uncertainty is represented by $\omega_1 \in \Omega_1$ and nonparametric uncertainty is represented by $\omega_2 \in \Omega_2$. The stationary elliptic partial differential equation representing the mean system of nonparametric uncertainty is affected by parametric uncertainty defined on the probability space $(\Omega_1, \mathcal{F}_1, P_1)$ with $\omega_1 \in \Omega_1$ such that

$$-\nabla.[a(\mathbf{r},\omega_1)\nabla u(\mathbf{r},\omega_1)] = f(\mathbf{r}); \quad \mathbf{r} \text{ in } \mathcal{D}; \quad u(\mathbf{r},\omega_1) = 0 \text{ on } \partial\mathcal{D} \tag{28}$$

where $\mathbf{r}$ denotes a point of the geometry, $a$ is a parameter depending on the material, $f$ is the source variable and $u$ is the primary variable. The solution procedure to this case using PC has already been discussed in Section 2.2. When considering nonparametric uncertainty, defined on $(\Omega_2, \mathcal{F}_2, P_2)$, the assumed knowledge of the system are the mean matrix and the dispersion parameter. If a system is known to have parametric uncertainty, the mean matrix of the combined model with respect to nonparametric uncertainty is given by the random matrix of the parametric uncertainty, that is

$$\mathrm{E}_2[\mathbf{K}_H] = \mathbf{K}_{Par} = p\boldsymbol{\Sigma} = \mathbf{K}_0 + \sum_{i=1}^{M} \xi_i \mathbf{K}_i \tag{29}$$

where $\mathrm{E}_2[\ ]$ denotes the mean taken with respect to $\Omega_2$, $\mathbf{K}_{Par}$ is the random matrix model only affected by parametric uncertainty, $\xi_i$ are independent identically distributed random variables defined on $(\Omega_1, \mathcal{F}_1, P_1)$. Parameter $p$ is defined in Eq. (25) where $\mathbf{G}_0 = \mathbf{K}_0$, that is, it is calculated as in the case where only nonparametric uncertainty affects the system so that $p = p(\Omega_2)$. The stiffness matrix considering combined uncertainty is then modelled by $\mathbf{K}_H \backsim W_n(p, (\mathbf{K}_0 + \sum \xi_i \mathbf{K}_i)/p)$. It is observed that, to perform MCS, firstly the parametric probabilistic space $(\Omega_1, \mathcal{F}_1, P_1)$ is sampled, and based on a particular sample of this space, the nonparametric probabilistic space $(\Omega_2, \mathcal{F}_2, P_2)$ is sampled. That is, when both spaces $(\Omega_1, \mathcal{F}_1, P_1)$ and $(\Omega_2, \mathcal{F}_2, P_2)$ are independent, the sample space is given by $\Omega_1 \times \Omega_2$.

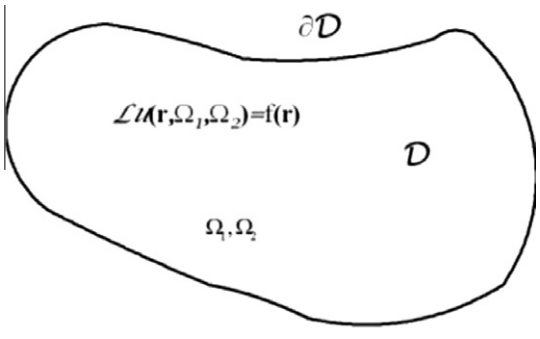


**Fig. 1.** Combined uncertainty over the entire domain.

### 4.2. Analytical solution

The solution of the problem is such that $\mathbf{u} = \mathbf{K}_H^{-1}\mathbf{f}$ with matrix $\mathbf{K}$ modelled by a Wishart matrix whose mean depends on a set of independent identically distributed random variables, that is, $\mathbf{K}_H \backsim W_n(p, (\mathbf{K}_0 + \sum \xi_i \mathbf{K}_i)/p)$. It is known from the theory of random matrices that the first and second moments of the inverse of a Wishart matrix $W_p(n, \boldsymbol{\Sigma})$, called inverted Wishart matrix, are given by [21] as

$$\mathrm{E}[\mathbf{W}^{-1}] = \frac{\boldsymbol{\Sigma}^{-1}}{p-n-1} \tag{30}$$

$$\mathrm{E}[\mathbf{W}^{-1}\mathbf{A}\mathbf{W}^{-1}] = c_1\boldsymbol{\Sigma}^{-1}\mathbf{A}\boldsymbol{\Sigma}^{-1} + c_2\left[\boldsymbol{\Sigma}^{-1}\mathbf{A}^T\boldsymbol{\Sigma}^{-1} + \mathrm{Trace}(\mathbf{A}\boldsymbol{\Sigma}^{-1})\boldsymbol{\Sigma}^{-1}\right] \tag{31}$$

with

$$c_1 = (p-n-2)c_2 \tag{32}$$

$$c_2 = 1/((p-n)(p-n-1)(p-n-3)) \tag{33}$$

Parametric and nonparametric uncertainties are assumed to be uncorrelated that is, the mean and the second moment of the response are given by

$$\mathrm{E}[\mathbf{u}] = \mathrm{E}_1[\mathrm{E}_2[\mathbf{u}]] = \frac{\mathrm{E}_1\left[\mathbf{K}_{Par}^{-1}\mathbf{f}\right]p}{p-n-1} \tag{34}$$

$$\mathrm{E}[\mathbf{u}\mathbf{u}^T] = \mathrm{E}_1[\mathrm{E}_2[\mathbf{u}\mathbf{u}^T]] = (c_1+c_2)p^2\mathrm{E}_1\left[\mathbf{K}_{Par}^{-1}\mathbf{F}\mathbf{K}_{Par}^{-1}\right] + c_2p^2\mathrm{E}_1 \times\left[\mathrm{Trace}(\mathbf{F}\mathbf{K}_{Par}^{-1})\mathbf{K}_{Par}^{-1}\right] \tag{35}$$

with $\mathbf{F} = \mathbf{f}\mathbf{f}^T$, and where $\mathrm{E}_1[\,]$ is the mean taken with respect to parametric uncertainty defined on $\Omega_1$. Means $\mathrm{E}_1\left[\mathbf{K}_{Par}^{-1}\right]$, $\mathrm{E}_1\left[\mathbf{K}_{Par}^{-1}\mathbf{F}\mathbf{K}_{Par}^{-1}\right]$ and $\mathrm{E}_1\left[\mathrm{Trace}(\mathbf{F}\mathbf{K}_{Par}^{-1})\mathbf{K}_{Par}^{-1}\right]$ will be expressed using the Polynomial Chaos expansion of the response obtained from the parametric uncertainty analysis using the Galerkin method. It is noted that non-intrusive methods (e.g., a collocation method) could also be used to approximate these means.

Denote by $\mathbf{u}^{(\mathrm{PC})}$, $\mathbf{K}_{Par}^{-1^{(\mathrm{PC})}}$ and $\mathbf{f}^{(\mathrm{PC})}$ the PC expansion of the system response, inverse of the parametric stiffness matrix and forcing term where only parametric uncertainty is considered. Then, the coefficients of the three PC expansions can be related through

$$\mathbf{u}^{(\mathrm{PC})} = \mathbf{K}_{Par}^{-1^{(\mathrm{PC})}}\mathbf{f}^{(\mathrm{PC})} \tag{36}$$

$$\mathbf{u}_k\mathrm{E}\left[\Gamma_k^2\right] = \sum_{i=1}^{P}\sum_{j=1}^{P}\mathbf{K}_i^{-1^{(\mathrm{PC})}}\mathbf{f}_j\mathrm{E}[\Gamma_i\Gamma_j\Gamma_k] \tag{37}$$

For $k = 1$, the first term of PC expansion of the response is given by $\mathbf{u}_1 = \sum_i \mathbf{K}_i^{-1^{(\mathrm{PC})}}\mathbf{f}_i\mathrm{E}\left[\Gamma_i^2\right]$. Then the PC expansion of $\mathbf{K}_{Par}^{-1^{(\mathrm{PC})}} = \sum_{i=1}^{P} \mathbf{K}_i^{-1^{(\mathrm{PC})}}\Gamma_i$ can be retrieved from the inverse of $\mathbf{A}^{(\mathrm{PC})}$, that is $(\mathbf{A}^{(\mathrm{PC})})^{-1}$, where $\mathbf{A}^{(\mathrm{PC})}$ is defined in Eq. (11). Denote by $\mathbf{A}^{(\mathbf{K}^{-1})}$ the matrix formed by the first $n$ rows of matrix $(\mathbf{A}^{(\mathrm{PC})})^{-1}$. Then $\mathbf{K}_i^{-1^{(\mathrm{PC})}} = \mathbf{A}_i^{(\mathbf{K}^{-1})}$ where $\mathbf{A}_i^{(\mathbf{K}^{-1})}$ is the $i$-th block of $n$ columns of $\mathbf{A}^{(\mathbf{K}^{-1})}$. Finally, the means appearing in Eqs. (34) and (35) are given by

$$\mathrm{E}_1[\mathbf{K}_{Par}^{-1}\mathbf{f}] = \mathrm{E}_1[\mathbf{u}^{(\mathrm{PC})}] = \mathbf{u}_1^{(\mathrm{PC})} \tag{38}$$

$$\mathrm{E}_1\left[\mathbf{K}_{Par}^{-1}\mathbf{F}\mathbf{K}_{Par}^{-1}\right] = \mathrm{E}_1[\mathbf{u}^{(\mathrm{PC})}(\mathbf{u}^{(\mathrm{PC})})^T] = \sum_{i=1}^{P}\mathbf{u}_i(\mathbf{u}_i)^T\mathrm{E}\left[\Gamma_i^2\right] \tag{39}$$

$$\mathrm{E}_1\left[\mathrm{Trace}\left(\mathbf{F}\mathbf{K}_{Par}^{-1}\right)\mathbf{K}_{Par}^{-1}\right] = \mathrm{E}_1\left[\mathrm{Trace}(\mathbf{f}(\mathbf{u}^{(\mathrm{PC})})^T)\mathbf{K}_{Par}^{-1}\right] = \sum_{i=1}^{P}\sum_{j=1}^{P}\sum_{k=1}^{P}(\mathbf{u}_i)^T\mathbf{f}_j\mathbf{K}_k^{-1^{(\mathrm{PC})}}\mathrm{E}[\Gamma_i\Gamma_j\Gamma_k]$$

The first and second moment of the response can then be approximated by

$$\mathrm{E}[\mathbf{u}] = \frac{\mathbf{u}_1^{(\mathrm{PC})}p}{(p-n-1)} \tag{40}$$

$$\mathrm{E}[\mathbf{u}\mathbf{u}^T] = (c_1+c_2)p^2\sum_{i=1}^{P}\mathbf{u}_i(\mathbf{u}_i)^T\mathrm{E}\left[\Gamma_i^2\right] + c_2p^2\sum_{i=1}^{P}\sum_{j=1}^{P}\sum_{k=1}^{P}(\mathbf{u}_i)^T\mathbf{f}_j\mathbf{K}_k^{-1^{(\mathrm{PC})}}\mathrm{E}[\Gamma_i\Gamma_j\Gamma_k] \tag{41}$$

The expressions obtaining the nonparametric moments are exact, and therefore the source of error is the PC approximation. The propagation of parametric uncertainty is an ongoing research topic, and improvements to the PC methods have been introduced by reducing the size of the matrices [43,44]. Also, other methods are available by projecting the stochastic partial differential equation in a different basis [6,7], or through the use of non-intrusive methods [36,7].

### 4.3. Numerical example: Euler Bernoulli beam

We first consider a simple 1D example from structural mechanics to illustrate the proposed method. The case of a clamped-free beam of length $L = 1.65$ m subjected to uniform distributed force $f = 1$ N/m is considered, as shown in Fig. 2. The system is modelled applying the Finite Element method to the Euler–Bernoulli equation using $n = 50$ elements, details on the method can be found, for example, in [45]. Parametric uncertainty is introduced in the system by a Gaussian random field $w(x,\theta) = EI_z$, and its mean is $\mu = \mathrm{E}[EI_z] = 5.7520$ N m$^2$. The discretization of $w(x,\theta)$ is done with the KL expansion of the exponential autocorrelation function $\mathrm{R}(x_1,x_2) = e^{-|x_1-x_2|/L}$, that is $w(x,\theta) = \sum_{i=1}^{\infty}\lambda_i\varphi_i\xi_i$ where the eigenvalues and eigenfunctions of the autocorrelation function $\lambda$, $\varphi(x_1)$ are obtained after solving the equation $\int_{-L/2}^{L/2}\mathrm{R}(x_1,x_2)\varphi(x_2)\,dx_2 = \lambda\varphi(x_1)$ and $\xi_i$ is a set of normal independent random variable, see [13] for more details. The KL expansion is truncated at $M = 2$, so that the corresponding KL expansion of the stiffness matrix is $\mathbf{K} = \mathbf{K}_0 + \mathbf{K}_1\xi_1 + \mathbf{K}_2\xi_2$, where the standard deviation of the random field is included in the $\mathbf{K}_i$ matrices. The maximum order of the Hermite polynomial used is 4, so that $P = 15$ polynomials are used as basis functions.

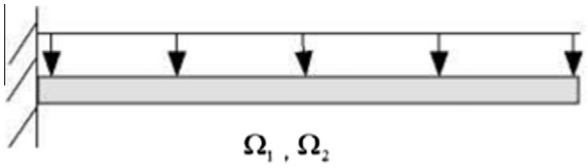


**Fig. 2.** Euler–Bernoulli beam with spatially varying random bending rigidity $w(x,\theta) = EI_z$ and nonparametric uncertainty affecting the whole domain. The length of the beam is $L = 1.65$ m, the section area is $A = 8.2123\times10^{-5}$ m$^2$, the density is $\rho = 7800$ kg/m$^3$ and the mean of the bending rigidity homogeneous random field is $\mu = 5.7520$ kg m$^2$.

The analytical expressions for mean and standard deviation can be obtained respectively from Eqs. (40) and (17) where the mean and second moment of the response can be obtained from Eqs. (40) and (41) respectively. The result of applying these expressions can be compared with Monte Carlo Simulation (MCS) results for different combinations of normalized standard deviations $\sigma/\mu$ of the random field and dispersion parameters $\delta$ of the Wishart matrix. The mean and standard deviation of the displacement for the case of $\delta = 0.05$ and $\sigma = 0.1\mu$ is given in Fig. 3. The mean and standard deviation of the tip displacement for different combinations of $\delta$ and $\sigma$ obtained with the proposed method are displayed in Fig. 4. The accuracy of the method is evaluated, through the error of the mean and standard deviation of tip displacement between the analytical expressions and MCS, in Fig. 5. MCS is performed both in Wishart matrix and parametric uncertainty, using 500 samples for Wishart matrices and 1000 samples for PC, resulting in 500 000 samples in total.

It is observed in Fig. 4(a) that the mean of the tip displacement varies both with the standard deviation of the random field and the dispersion parameter of the random matrix. This observation can be extended to the standard deviation in Fig. 4(b), where the effect of $\sigma/\mu$ is more important than the one of $\delta$ in comparison to the results obtained for mean. With respect to the error of both quantities, it is observed that the error does not depend strongly on $\delta$, as it is almost constant for each normalized standard deviation of the random field. It is also observed in Fig. 5(a) that the error of both mean and standard deviation grow with $\sigma/\mu$.

### 4.4. Numerical example: flow through porous media

In the previous subsection, a 1D example was given, now the efficiency of the method for a 2D example is perused. A numerical example of flow through porous media is now considered to show the efficiency of the proposed method. The two-dimensional domain considered is a rectangle of length $L = 0.998$ m and width $W = 0.59$ m, as shown in Fig. 6. The domain is divided with a uniform mesh of $25\times15$ rectangular elements. The porous medium within the domain is subjected to a constant source of strength $q_b = 1$ kg/cm$^3$s along the portion of its boundary where $y = -0.2950$ m and $x \in [0.2994, 0.4990]$ m. The head is fixed at value $h_b = 0$ cm along the portion of the boundary such that $x = -0.4990$ m, $y \in [0.1770, 0.2950]$ m. The deterministic system has $n = 412$ degrees of freedom. A Gaussian hydraulic conductivity ($k$) with 2D exponential autocorrelation function is considered. The 2D autocorrelation function is obtained as the product of two 1D exponential autocorrelation functions, the first one depending on $x$, with correlation length $b_x = L$; and the second one depending on $y$, with correlation length $b_y = W$. Two terms of the KL expansion in each direction are kept, that is, the KL expansion has four matrices for the whole system. The mean value of the constant appearing in the PDE modelling the system, i.e., squared of the density multiplied by the hydraulic conductivity and the gravitational acceleration and divided by the permeability is given by $\bar{k} = 1kg$ cm$^2$/s. The stiffness element matrices are given by

$$\mathbf{K}_{I_i}^{(e)} = \int_0^a\int_0^b a_{11}\frac{d\mathbf{N}^{(e)}}{dx}\frac{d\mathbf{N}^{(e)}}{dx}(\varphi(x)\varphi(y))_i\,dx\,dy \tag{42}$$

$$\mathbf{K}_{II_i}^{(e)} = \int_0^a\int_0^b a_{22}\frac{d\mathbf{N}^{(e)}}{dy}\frac{d\mathbf{N}^{(e)}}{dy}(\varphi(x)\varphi(y))_i\,dx\,dy \tag{43}$$

The stiffness matrix of the system is given by $\mathbf{K} = \mathbf{K}_I + \mathbf{K}_{II}$, where $\mathbf{K}_I$ and $\mathbf{K}_{II}$ are obtained by assembling the respective matrices given above. The details of the Finite Element model can be found, for example, in [46]. The 2D eigenfunction $(\varphi(x)\varphi(y))_i$ is the product of two 1D eigenfunctions of the KL expansion of the exponential autocorrelation function, knowing that only two eigenfunctions

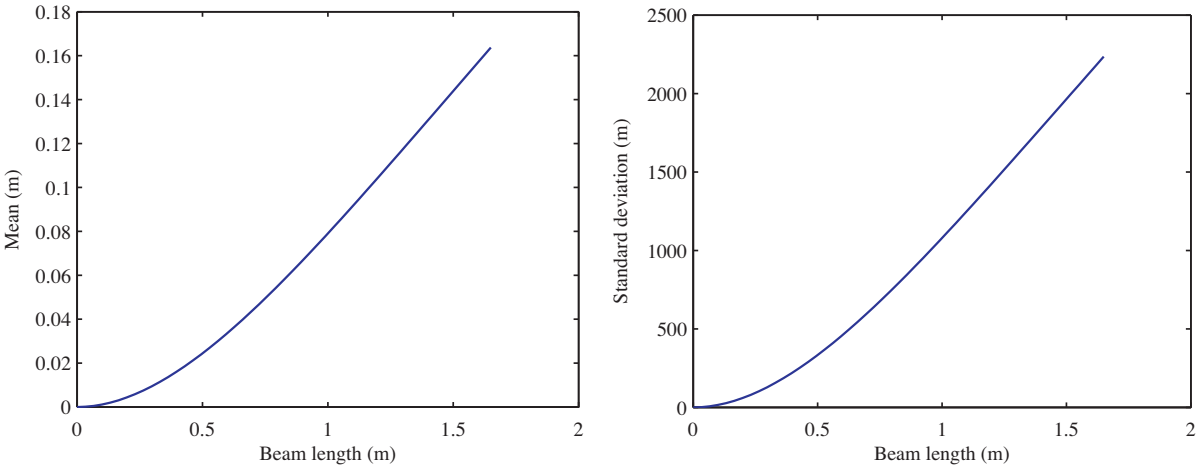


(a) Mean. (b) Standard deviation.

**Fig. 3.** Mean and standard deviation of the vertical displacement obtained using the proposed analytical expressions for $\delta = 0.05$ and $\sigma = 0.1\mu$.

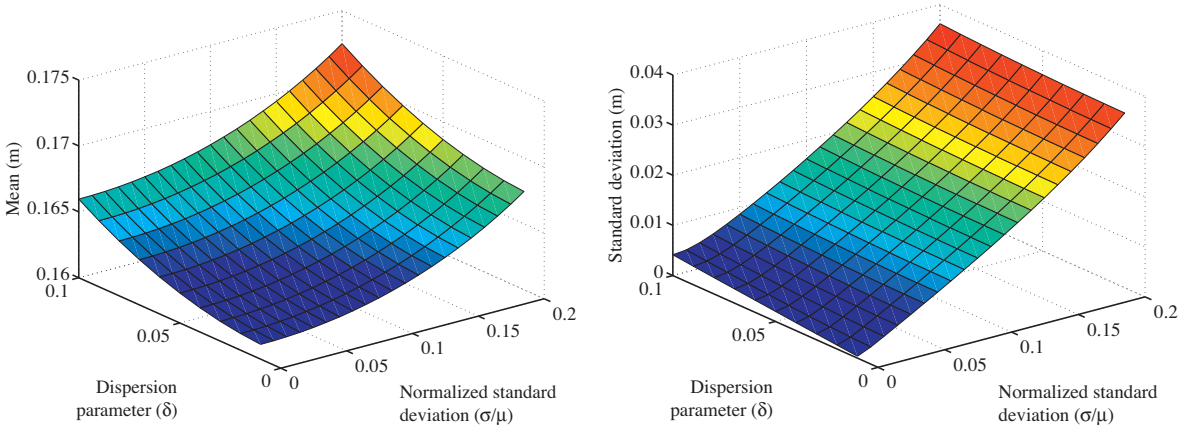


(a) Mean. (b) Standard deviation.

**Fig. 4.** Mean and standard deviation of the tip vertical displacement obtained using the proposed analytical expressions for different values of dispersion parameter ($\delta$) and normalized standard deviation ($\sigma/mu$).

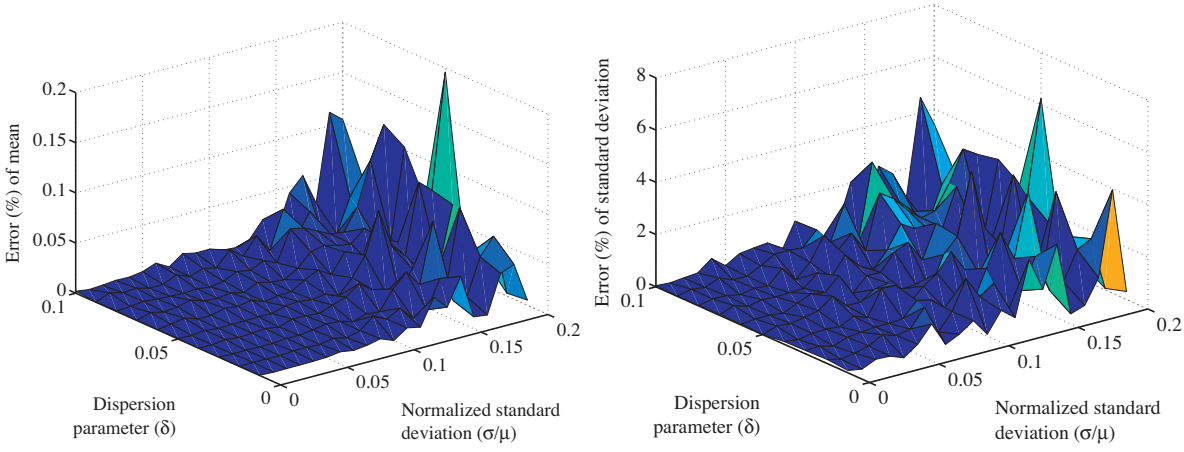


(a) Percentage error of mean. (b) Percentage error of standard deviation.

**Fig. 5.** Percentage error of mean and standard deviation of the tip vertical displacement between the analytical expressions and Monte Carlo Simulation (MCS) using 500 000 samples, for different values of dispersion parameter ($\delta$) and normalized standard deviation ($\sigma/mu$).

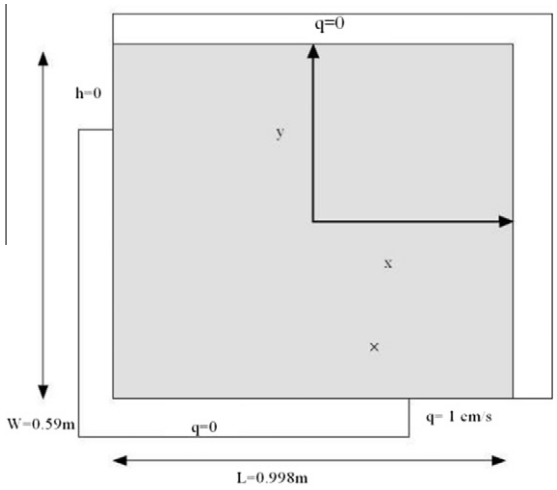


**Fig. 6.** Flow through a rectangular porous media. The porous media is assumed to have stochastically inhomogeneous hydraulic conductivity. The point at which the mean and standard deviation obtained with analytical expressions and MCS are compared is shown by $\times$.

are kept in each direction. The random variables appearing in the stiffness matrix are $a_{11} = a_{22} = k$. The eigenfunction $\varphi(x,y) = 1$ for the deterministic stiffness matrix, and it depends on the autocorrelation function when considering a KL expansion matrix. Parametric uncertainty is dealt with using a fourth-order polynomial chaos, so that the total number of polynomials is 70.

The analytical expressions for the mean, given by Eq. (40), and standard deviation, given by Eq. (17) where the mean and second moment of the response can be obtained from Eqs. (40) and (41) respectively, are applied and compared with MCS results for different combinations of normalized standard deviations $\sigma/\mu$ of the random field and dispersion parameters $\delta$ of the Wishart matrix. The mean and standard deviation of the head obtained with the proposed method for $\sigma = 0.1$ and $\delta = 0.05$ are displayed in Fig. 7. The same results for the point situated at $(x,y) = (0.6786, 0.0393)$ and different combinations of $\sigma/\mu$ and $\delta$ are shown in Fig. 8. The choice of this point is for illustration only, the method proposed here is applicable to all points of the domain. The accuracy of the method is evaluated through the error of the mean and standard deviation of the head at this point, in Fig. 9. MCS is performed both in Wishart matrix and parametric uncertainty, using 100 samples for Wishart matrices and 1000 samples for the random field, so that the total number of samples used is 100000. It is observed in Fig. 8(a) that the mean of the tip displacement increases both with the standard deviation of the random field and the dispersion parameter of the random matrix, where the effect of the dispersion parameter is more important than the effect of the normalized standard deviation. The standard deviation displayed in Fig. 8(b) also increases with both parameters, but the the effect of $\sigma/\mu$ is more important than the one of $\delta$. With respect to the error of both quantities, it is observed that the error does not depend on $\delta$, as it is maintained almost constant for each normalized standard deviation of the random field. It is also observed in Fig. 5(a) that the error of is also close to constant with respect to $\sigma/\mu$. The percentage error for standard deviation seems to increase with $\sigma/\mu$. Both errors are of lower order than the ones obtained for the beam problem.

## 5. Combined uncertainty over non-overlapping subdomains

### 5.1. Problem description

Combined uncertainty over different domains arises, for example, when a structure is constituted of several parts where some of them are accurately modeled through parametric uncertainty and the behavior of the remaining substructures is not well understood and therefore can be modelled with nonparametric uncertainty. This situation arises, for example, in the wing of a plane with engines attached to it, where the wing could be modeled with parametric uncertainty and the engines with nonparametric uncertainty due to the complexity of the substructure. Several substructuring techniques are available in the literature [47]. Domain decomposition and FETI-based methods have been applied for the case of parametric uncertainty affecting the whole domain [48,49]. In this section, the case where each kind of uncertainty (parametric and nonparametric) affects a different subdomain of the structure is considered.

### 5.2. Proposed solution procedure

In Fig. 10, two probability spaces are considered, $(\Omega_j, \mathcal{F}_j, P_j)$ for $j = 1,2$, each one affecting the system on the subdomain $\mathcal{D}_j$ of $\mathcal{D}$, such that $\mathcal{D}_1 \bigcup \mathcal{D}_2 = \mathcal{D}$, $\mathcal{D}_1 \bigcap \mathcal{D}_2 = \varnothing$ and $\Gamma$ is the boundary

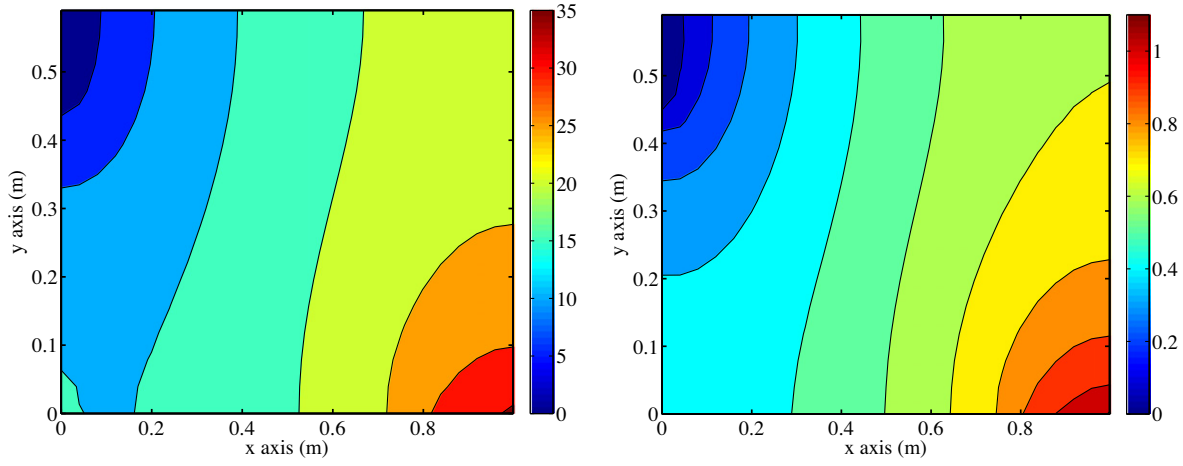


(a) Mean. (b) Standard deviation.

**Fig. 7.** Mean and standard deviation of the head, in cm, obtained using the proposed analytical expressions for $\sigma = 0.1$ and $\delta = 0.05$.

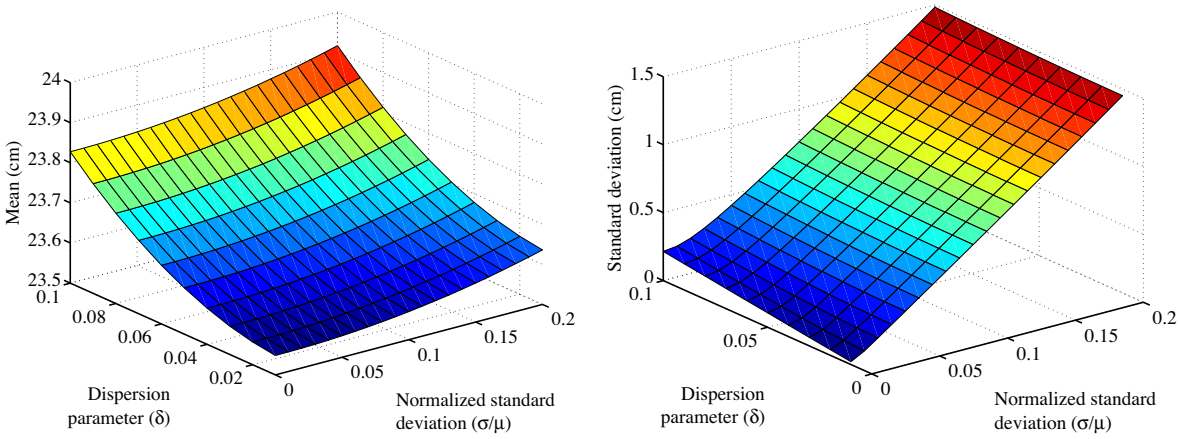


(a) Mean. (b) Standard deviation.

**Fig. 8.** Mean and standard deviation of the head at $(x,y) = (0.6786, 0.0393)$ obtained using the proposed analytical expressions, for different values of dispersion parameter ($\delta$) and normalized standard deviation ($\sigma/\mu$).

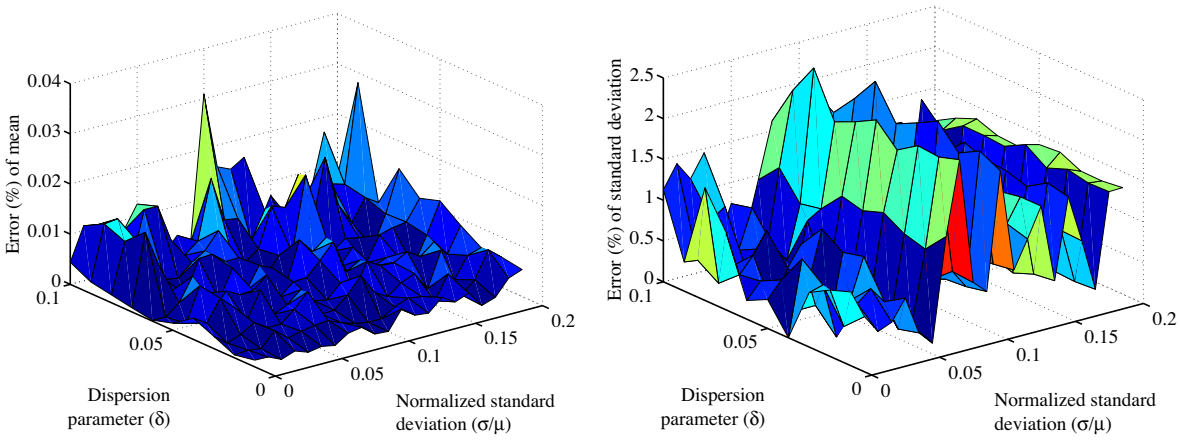


(a) Percentage error of mean. (b) Percentage error of standard deviation.

**Fig. 9.** Percentage error of mean and standard deviation of the head at $(x,y) = (0.6786, 0.0393)$ between the analytical expressions and Monte Carlo Simulation (MCS) using 100 000 samples, for different values of dispersion parameter ($\delta$) and normalized standard deviation ($\sigma/\mu$).

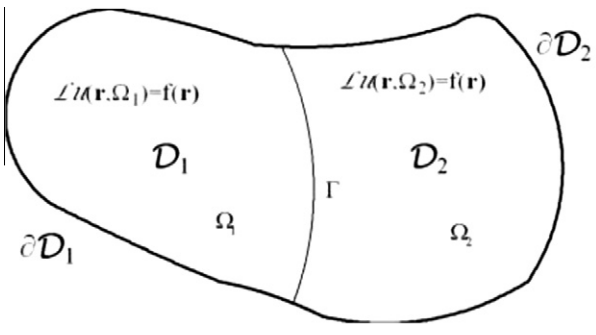


**Fig. 10.** Combined uncertainty over non-overlapping domain.

between the two subdomains. The case of an elliptic partial differential equation with a Dirichlet boundary condition is considered, where the equation is affected by parametric uncertainty defined on $(\Omega_1, \mathcal{F}_1, P_1)$ and by nonparametric uncertainty defined on $(\Omega_2, \mathcal{F}_2, P_2)$. The parametric uncertainty is firstly introduced in the elliptic partial differential Eq. (28) First consider domain $\mathcal{D}_2$ is deterministic. The finite element method can be applied, where the random field used to model the parameter $a(\mathbf{r},\omega_1)$ is expanded with the KL expansion. The elliptic partial differential equation with parametric uncertainty in subdomain $\mathcal{D}_1$ leads to the algebraic equation

$$\begin{bmatrix} [\mathbf{K}_{11_0} + \sum_{i=1}^{M} \xi_i(\theta)\mathbf{K}_{11_i}] & [\mathbf{K}_{12}] \\ [\mathbf{K}_{21}] & [\mathbf{K}_{22}] \end{bmatrix} \begin{bmatrix} \mathbf{u}_I(\Omega_1) \\ \mathbf{u}_{II}(\Omega_1) \end{bmatrix} = \begin{bmatrix} \mathbf{f}_I(\Omega_1) \\ \mathbf{f}_{II}(\Omega_1) \end{bmatrix}. \tag{44}$$

Here, response and forcing vectors can be expanded with PC such that the response and force for nodes in $\mathcal{D}_1$ are given by $\mathbf{u}_I = \sum_{j=1}^{P} \mathbf{u}_{Ij}\Psi_j(\Omega_1)$ and $\mathbf{f}_I = \sum_{j=1}^{P} \mathbf{f}_{Ij}\Psi_j(\Omega_1)$, and the response and force for nodes in $\mathcal{D}_2$ are $\mathbf{u}_{II} = \sum_{j=1}^{P} \mathbf{u}_{IIj}\Psi_j(\Omega_1)$ and $\mathbf{f}_{II} = \sum_{j=1}^{P} \mathbf{f}_{IIj}\Psi_j(\Omega_1)$. The vectors $\mathbf{u}_{Ij}$ and $\mathbf{u}_{IIj}$ can be retrieved by applying Galerkin method to Eq. (44) or through numerical integration. The vectors $\mathbf{u}_{1j}$ resulting from applying Galerkin method, that is, multiplying Eq. (44) by each basis function $\Gamma_p$ and taking mean, are obtained from the solution of the deterministic linear system

$$\widehat{\mathbf{K}}\begin{bmatrix}\mathbf{u}_{I1}\\ \vdots \\ \mathbf{u}_{IIP}\end{bmatrix}=\begin{bmatrix}\mathbf{f}_{I1}-\mathbf{K}_{12}\mathbf{K}_{22}^{-1}\mathbf{f}_{II1}\\ \vdots \\ \mathbf{f}_{IP}-\mathbf{K}_{12}\mathbf{K}_{22}^{-1}\mathbf{f}_{IIP}\end{bmatrix} \tag{45}$$

where

$$\widehat{\mathbf{K}}=\mathbf{d}\otimes\left(\mathbf{K}_{11_0}-\mathbf{K}_{12}\mathbf{K}_{22}^{-1}\mathbf{K}_{21}\right)+\sum_{i=1}^{M}\mathbf{c}_i\otimes\mathbf{K}_{11_i} \tag{46}$$

and vector of coefficients $\left[\mathbf{u}_{II1}^T,\ldots,\mathbf{u}_{IIP}^T\right]^T$ can be related to coefficients $\left[\mathbf{u}_{I1}^T,\ldots,\mathbf{u}_{IP}^T\right]^T$ through

$$\begin{bmatrix}\mathbf{u}_{II1}\\ \vdots \\ \mathbf{u}_{IIP}\end{bmatrix}=\begin{bmatrix}\mathbf{K}_{22}^{-1}(\mathrm{E}[\Psi_1,\mathbf{f}_{II}]-\mathbf{K}_{12}\mathbf{u}_{I1})\\ \vdots \\ \mathbf{K}_{22}^{-1}(\mathrm{E}[\Psi_P,\mathbf{f}_{II}]-\mathbf{K}_{12}\mathbf{u}_{IP})\end{bmatrix} \tag{47}$$

Alternatively, vectors $\mathbf{u}_{Ij}$ can be obtained using Eq. (13), where each response $\mathbf{u}_{Ij}(\xi_{1j_1}\ldots\xi_{Mj_M})$ used for the quadrature is obtained through

$$\mathbf{u}_{Ij}(\xi_{1j_1}\ldots\xi_{Mj_M})=\left(\mathbf{K}_{11_0}-\mathbf{K}_{12}\mathbf{K}_{22}^{-1}\mathbf{K}_{21}+\sum_{i=1}^{M}\xi_{ij_i}\mathbf{K}_{11_i}\right)^{-1}\left(\mathbf{f}_I-\mathbf{K}_{12}\mathbf{K}_{22}^{-1}\mathbf{f}_{II}\right) \tag{48}$$

The vector of coefficients $\left[\mathbf{u}_{II1}^T,\ldots,\mathbf{u}_{IIP}^T\right]^T$ can be related to coefficients $\left[\mathbf{u}_{I1}^T,\ldots,\mathbf{u}_{IP}^T\right]^T$ through Eq. (47). Model uncertainty, represented by $(\Omega_2,\mathcal{F}_2,P_2)$ affects the subdomain $\mathcal{D}_2$ and can be included in the algebraic Eq. (44) through submatrix $\mathbf{K}_{22}(\Omega_2)$. This type of uncertainty can only be considered after calculating the system matrix, as it is part of the information used to find the matrix pdf

$$\begin{bmatrix}\left[\mathbf{K}_{11_0}+\sum_{i=1}^{M}\xi_i(\theta)\mathbf{K}_{11_i}\right] & [\mathbf{K}_{12}]\\ [\mathbf{K}_{21}] & [\mathbf{K}_{22}(\Omega_2)]\end{bmatrix}\begin{bmatrix}\sum_{j=1}^{P}\mathbf{u}_{Ij}(\Omega_2)\Psi_j(\Omega_1)\\ \sum_{j=1}^{P}\mathbf{u}_{IIj}(\Omega_2)\Psi_j(\Omega_1)\end{bmatrix}=\begin{bmatrix}\sum_{j=1}^{P}\mathbf{f}_{Ij}\Psi_j(\Omega_1)\\ \sum_{j=1}^{P}\mathbf{f}_{IIj}\Psi_j(\Omega_1)\end{bmatrix} \tag{49}$$

The global matrix has to remain positive definite. This is not satisfied for any positive definite matrix $\mathbf{K}_{22}(\Omega_2)$. Two methods are proposed in the next two subsections to model $\mathbf{K}_{22}$ using a Wishart random matrix such that positive definiteness of the global matrix is satisfied. Once the samples $\mathbf{K}_{22}(\Omega_2)$ are obtained, vectors $\mathbf{u}_{Ij}$, $\mathbf{u}_{IIj}$ are obtained from Eqs. (49) and (47). The mean and second moments of the response are then retrieved

$$\mathrm{E}[\mathbf{u}_I]=\mathrm{E}_2[\mathrm{E}_1[\mathbf{u}_I]]=\mathrm{E}_2[\mathbf{u}_{I1}] \tag{50}$$

$$\mathrm{E}\left[\mathbf{u}_I\mathbf{u}_I^T\right]=\mathrm{E}_2\left[\mathrm{E}_1\left[\mathbf{u}_I\mathbf{u}_I^T\right]\right]=\mathrm{E}_2\left[\sum_{j=1}^{P}\mathbf{u}_{Ij}\mathbf{u}_{Ij}^T\mathrm{E}\left[\Gamma_j^2\right]\right]=\sum_{j=1}^{P}\mathrm{E}_2\left[\mathbf{u}_{Ij}\mathbf{u}_{Ij}^T\right]\mathrm{E}\left[\Gamma_j^2\right] \tag{51}$$

The same expressions are valid to retrieve the moments of $\mathbf{u}_{II}$ by changing the subindex $I$ to $II$.

### 5.2.1. Ensuring positive definiteness through sample selection

Submatrix $\mathbf{K}_{22}(\Omega_2)$ is modelled using the maximum entropy principle exposed in Section 3, leading to the distribution of a Wishart random matrix. This distribution is conditional on the global matrix being positive definite, that is, for every sample of $\mathbf{K}_{22}(\Omega_2)$, the matrix from Eq. (49) has to be positive definite. It is assumed that this is satisfied for a particular sample of $\mathbf{K}_{22}(\Omega_2)$ and for all samples of $\xi_i$ if the matrix

$$\begin{bmatrix}\mathbf{K}_{11_0}-C\sum_{i=1}^{M}\mathbf{K}_{11_i} & \mathbf{K}_{12}\\ \mathbf{K}_{21} & \mathbf{K}_{22}(\Omega_2)\end{bmatrix} \tag{52}$$

is positive definite. This assumption implies that the upper diagonal block matrix is positive definite $\mathbf{K}_{11_0}-C\sum_{i=1}^{M}\mathbf{K}_{11_i}>0$. Heuristically, we can observe that, if matrices $\mathbf{K}_{11_0}$ and $\mathbf{K}_{11_i}$ are scalar, $\mathbf{K}_{11_0}+\sum_{i=1}^{M}\xi_i\mathbf{K}_{11_i}$ reduces to a Gaussian random variable, so that $\xi_i=-4\sqrt{\left(\sum_{i=1}^{M}\mathbf{K}_{11_i}^2\right)}$ implies that 99.99% of the samples of this random variable lead to larger values than $\mathbf{K}_{11_0}-4\sum_{i=1}^{M}\mathbf{K}_{11_i}$. That is, if we want $\mathbf{K}_{11_0}+\sum_{i=1}^{M}\xi_i\mathbf{K}_{11_i}>0$, introducing $C=4$ in Eq. (52) is likely to lead to a positive definite upper diagonal submatrix. In other words, we can consider the global matrix from Eq. (49) as the sum of a positive definite matrix and $M$ non-negative definite matrices

$$\begin{bmatrix}\left[\mathbf{K}_{11_0}+\sum_{i=1}^{M}\xi_i(\theta)\mathbf{K}_{11_i}\right] & [\mathbf{K}_{12}]\\ [\mathbf{K}_{21}] & [\mathbf{K}_{22}(\Omega_2)]\end{bmatrix}=\begin{bmatrix}\mathbf{K}_{11_0}-C\sum_{i=1}^{M}\mathbf{K}_{11_i} & \mathbf{K}_{12}\\ \mathbf{K}_{21} & \mathbf{K}_{22}(\Omega_2)\end{bmatrix}+\begin{bmatrix}\sum_{i=1}^{M}(\xi_i+C)\mathbf{K}_{11_i} & 0\\ 0 & 0\end{bmatrix} \tag{53}$$

so that the global matrix is positive definite.

Both uncertainties are assumed independent and propagation of the parametric uncertainty is solved with PC. The equations related to the PC chosen method, i.e., Eqs. (45) and (47) for Galerkin method and Eqs. 13, 48 and 47 for numerical integration, are solved for each sample of the random matrix $\mathbf{K}_{22}(\Omega_2)$. First and second moments of $\mathbf{u}$ are obtained through MCS, where $\mathbf{K}_{22}\backsim W_n(p,\mathrm{E}[\mathbf{K}_{22}]/p)$ is simulated and the only samples used are the ones leading to a positive definite matrix in Eq. (52).

It is noted that with this method $\mathbf{K}_{22}$ does not have a Wishart distribution as some samples of the Wishart distribution will be rejected, namely the ones leading to a nonpositive definite matrix in Eq. (52).

### 5.2.2. Ensuring positive definiteness through matrix correction

The system matrix from Eq. (49) has to be positive definite. As formerly, it is assumed that if the sample $\left[\mathbf{K}_{11_0}-C\sum_{i=1}^{M}\mathbf{K}_{11_i}\right]$ of the KL expansion leads to a positive definite matrix upper diagonal matrix, other samples of $\xi_i$ will lead to matrix $\mathbf{K}_{11_0}+\sum_{i=1}^{M}\xi_i(\Omega_1)\mathbf{K}_{11_i}$ being positive definite. The global matrix considering only nonparametric uncertainty, i.e., substituting parametric uncertainty by the proposed sample, can be obtained through

$$\begin{bmatrix}[\mathbf{K}_{11_0}-C\sum_{i=1}^{M}\mathbf{K}_{11_i}] & [\mathbf{K}_{12}]\\ [\mathbf{K}_{21}] & [\mathbf{K}_{22}(\Omega_2)]\end{bmatrix}=\begin{bmatrix}[\mathbf{I}] & [\mathbf{O}]\\ [\mathbf{A}] & [\mathbf{I}]\end{bmatrix}\begin{bmatrix}[\mathbf{K}_{11_0}-C\sum_{i=1}^{M}\mathbf{K}_{11_i}] & [\mathbf{O}]\\ [\mathbf{O}] & [\mathbf{W}(\Omega_2)]\end{bmatrix}\begin{bmatrix}[\mathbf{I}] & [\mathbf{A}^T]\\ [\mathbf{O}] & [\mathbf{I}]\end{bmatrix} \tag{54}$$

with $\mathbf{W}$ a Wishart matrix. Matrices $[\mathbf{K}_{11_0}-C\sum_{i=1}^{M}\mathbf{K}_{11_i}]$ and $\mathbf{W}$ are positive definite, so that the resulting matrix will be positive definite [50]. Identifying terms we obtain

$$\mathbf{A}=\mathbf{K}_{21}\left(\mathbf{K}_{11_0}-C\sum_{i=1}^{M}\mathbf{K}_{11_i}\right)^{-1} \tag{55}$$

$$\mathbf{W}=\mathbf{K}_{22}-\mathbf{K}_{21}\left(\mathbf{K}_{11_0}-C\sum_{i=1}^{M}\mathbf{K}_{11_i}\right)^{-1}\mathbf{K}_{12} \tag{56}$$

where $\mathbf{W}$ is modelled as a Wishart matrix. Therefore, matrix $\mathbf{W}$ is such that


**Fig. 11.** Euler–Bernoulli beam with spatially varying random bending rigidity $w(x,\theta) = EI_z$ and nonparametric uncertainty affecting the different subdomains. The length of the beam is $L = 1.65$ m, the section area is $A = 8.2123 \times 10^{-5}$ m$^2$, the density is $\rho = 7800$ kg/m$^3$ and the mean of the bending rigidity random field is $\mu = \mathrm{E}[w(\theta,x)] = 5.7520$ kg m$^2$. The length of the domain affected by parametric uncertainty ($\Omega_1$) is $L_r = 0.792$ m.

$$\mathrm{E}[\mathbf{W}] = \mathrm{E}[\mathbf{K}_{22}] - \mathbf{K}_{21}\left(\mathbf{K}_{11_0} - C\sum_{i=1}^{M}\mathbf{K}_{11_i}\right)^{-1}\mathbf{K}_{12} \tag{57}$$

and the dispersion parameter is calculated as formerly, as matrix $\mathbf{K}_{21}\left(\mathbf{K}_{11_0} - C\sum_{i=1}^{M}\mathbf{K}_{11_i}\right)^{-1}\mathbf{K}_{12}$ is constant and does not introduce uncertainty in submatrix $\mathbf{K}_{22}$. The PC expansion of the response can now be calculated as in the previous subsection, from Eqs. (45) and (47) for Galerkin method and Eqs. (13), (48) and (47) for numerical integration, where $\mathbf{K}_{22}(\Omega_2)$ is now simulated as the sum of a Wishart matrix $\mathbf{W}(\Omega_2)$ and a constant matrix $\mathbf{K}_{21}\left(\mathbf{K}_{11_0} - C\sum_{i=1}^{M}\mathbf{K}_{11_i}\right)^{-1}\mathbf{K}_{12}$. As in the previous subsection, $C = 4$ is assumed.

### 5.3. Numerical example: Euler Bernoulli beam

The proposed method is firstly illustrated with a 1D problem. The case of a clamped-free beam of length $L = 1.65$ m subjected to uniform distributed force $f = 1$ N/m is considered, as described in Fig. 11. The system is modelled applying the Finite Element method to the Euler–Bernoulli equation using $n = 50$ elements, details on the method can be found, for example, in [45]. Parametric uncertainty is introduced in the system by an homogeneous Gaussian random field $w(\theta,x) = EI_z$ of mean $\mu = \mathrm{E}[EI_z] = 5.7520$ N m$^2$. This uncertainty affects the submatrix corresponding to the length of the beam $L_r = 0.792$ m closer to the clamped boundary. The discretization of $w(x,\theta)$ is done with the KL expansion of the exponential autocorrelation function $\mathrm{R}(x_1,x_2) = e^{-|x_1-x_2|/L_r}$. The KL expansion is truncated at $M = 2$, so that the corresponding KL expansion of the stiffness matrix is $\mathbf{K} = \mathbf{K}_0 + \sum_{i=1}^{2}\mathbf{K}_i\xi_i$, where the standard deviation of the random field is included in the $\mathbf{K}_i$ matrices. The maximum order of the Hermite polynomial used is 4, so that $P = 15$ polynomials are used as basis functions. The accuracy of the methods is evaluated through the error of the mean and standard deviation of tip displacement for different standard deviations of the random field ($\sigma/\mu \in (0,0.15)$) and dispersion parameters of the Wishart matrix ($\delta \in (0,0.1)$).

#### 5.3.1. Sample selection

The beam problem is solved using the method proposed in Section 5.2.1. Fig. 12 shows the error between results from Eqs. (45) and (47), where Wishart matrices are simulated with MCS using 500 samples, and MCS both in Wishart matrix and parametric uncertainty, using 500 samples for Wishart matrix results and 2000 samples for PC results within each Wishart sample, that is, a total of 1 000 000 samples. In Fig. 12(a) and (b) it is observed that both errors in mean and standard deviation increase with the normalized standard deviation. It is also observed that, compared to the case of both kinds of uncertainty over the same domain, the errors obtained for this example are around one tenth of the previous ones.

#### 5.3.2. Matrix correction

The beam problem is solved using the method exposed in Section 5.2.2. Fig. 13 shows the error between results from Eqs. (45) and (47), where Wishart matrices are simulated with MCS using 500 samples, and MCS both in Wishart matrix and parametric uncertainty, using 500 samples for Wishart matrix results and 2000 samples for PC results within each Wishart sample, that is, a total of 1 000 000 samples. In Fig. 13(a) and (b) it is observed that, as in the previous case, both errors in mean and standard deviation increase with the normalized standard deviation.

### 5.4. Numerical example: flow through porous media

The proposed methods are now applied to a 2D problem. An example of flow through a porous media is considered to show the efficiency of the proposed method. The two-dimensional domain is a rectangle of length $L = 0.998$ m and width $W = 0.59$ m, where the top half of the domain is affected by nonparametric

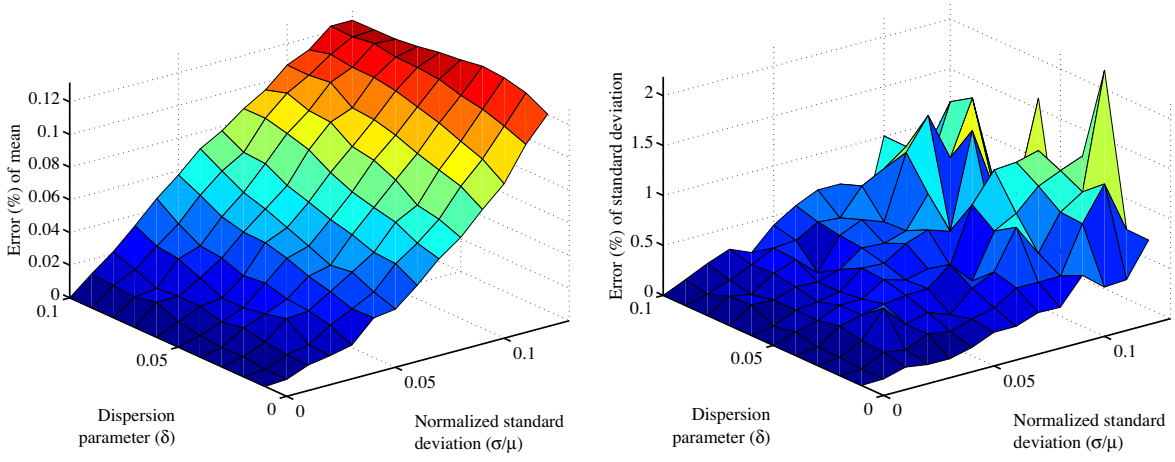


(a) Percentage error of mean. (b) Percentage error of standard deviation.

**Fig. 12.** Percentage error of mean and standard deviation of the tip vertical displacement between the analytical expressions for parametric uncertainty and Monte Carlo Simulation (MCS), for different values of the dispersion parameter $\delta$ and the normalized standard deviation $\sigma/\mu$, where positive definiteness of the global matrix is ensured through a sample selection procedure.

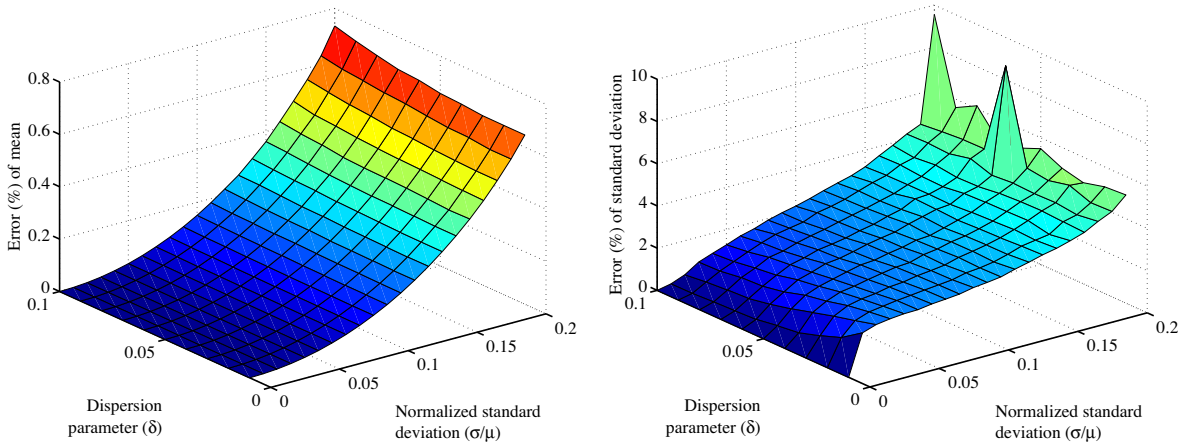


(a) Percentage error of mean. (b) Percentage error of standard deviation.

**Fig. 13.** Percentage error of mean and standard deviation of the tip vertical displacement between the analytical expressions for parametric uncertainty and Monte Carlo Simulation (MCS), for different values of the dispersion parameter $\delta$ and the normalized standard deviation $\sigma/\mu$, where positive definiteness of the global matrix is ensured through a matrix correction procedure.

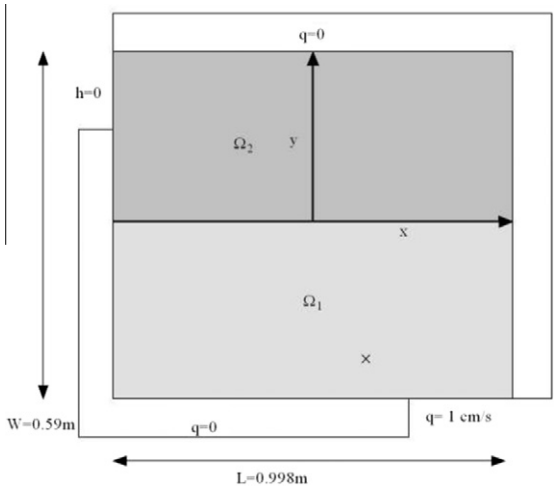


**Fig. 14.** Flow through a rectangular porous media. The porous media is assumed to have stochastically inhomogeneous hydraulic conductivity. The point at which the mean and standard deviation obtained with analytical expressions and MCS are compared is shown by $\times$.

uncertainty and the top bottom by parametric uncertainty, as shown in Fig. 14.

The domain is divided with a uniform mesh of $25 \times 15$ rectangular elements and is subjected to a constant source of strength $q_b = 1$ kg/cm$^3$ s along the portion of its boundary comprising the last 0.1996 m in $x$ direction. The head is fixed at value $h_b = 0$ cm along the portion of the boundary comprising the last 0.118 m in $y$ direction. The deterministic system has $n = 412$ degrees of freedom. A Gaussian hydraulic conductivity ($k$) with 2D exponential autocorrelation function is considered for the rectangular domain affecting the bottom 7 elements in $y$ direction. The 2D autocorrelation function is obtained as the product of two 1D exponential autocorrelation functions, the first one depending on $x$, with correlation length $b_x = L$; and the second one depending on $y$, with correlation length $b_y = W7/15$. Two terms of the KL expansion in each direction are kept, that is, the KL expansion has four matrices for the subdomain affected by parametric uncertainty. The mean value of the constant appearing in the PDE modelling the system, i.e., squared of the density multiplied by the hydraulic conductivity and the gravitational acceleration and divided by the permeability is given by $\overline{k} = 1$ kg cm$^2$/s. The stiffness element matrices are given by Eq. (42), where $\mathbf{K} = \mathbf{K}_{11} + \mathbf{K}_{22}$, $a_{11} = a_{22} = k$. The eigenfunction $\varphi(x,y)$ in that equation is one for the deterministic case and depends on the autocorrelation function when considering a KL expansion matrix. Parametric uncertainty is dealt with using a fourth-order polynomial chaos, so that the total number of polynomials is 70.

### 5.4.1. Sample selection

The flow problem is solved using the method proposed in Section 5.2.1. Fig. 15 shows the mean and standard deviation of the head for $\sigma = 0.1$ of the underlying random field and $\delta = 0.05$ for the nonparametric uncertainty, using PC to solve parametric uncertainty and MCS with 100 samples to solve nonparametric uncertainty. Fig. 16 shows the mean and standard deviation obtained from Eqs. (45) and (47), where Wishart matrices are simulated with MCS using 100 samples. Fig. 17 shows the error between results from Eqs. (45) and (47), where Wishart matrices are simulated with MCS using 100 samples, and MCS both in Wishart matrix and parametric uncertainty, using 100 samples for Wishart matrix results and 100 samples for PC results within each Wishart sample. These mean, standard deviation and errors are given for the head at coordinate $(x,y) = (0.6923, 0.0400)$.

In Fig. 16(a) and (b) it is observed that both the mean and standard deviation increase drastically with $\delta$, so that the variation with $\sigma/\mu$ seems negligible in comparison. In Fig. 17(a) and (b) it is observed that the error in mean and standard deviation vary mostly with $\sigma/\mu$, as the dependance with nonparametric uncertainty has been calculated with MCS. The errors are small in comparison with the ones obtained for the beam problem.

### 5.4.2. Matrix correction

The flow problem is solved using the method proposed in Section 5.2.2. Fig. 18 shows the mean and standard deviation of the head for $\sigma = 0.1$ of the underlying random field and $\delta = 0.05$ for the nonparametric uncertainty, using PC to solve parametric uncertainty and MCS with 100 samples to solve nonparametric uncertainty. Fig. 19 shows the results from Eqs. (45) and (47), where Wishart matrices are simulated with MCS using 500 samples. Fig. 20 shows the error between results from Eqs. (45) and (47), where Wishart matrices are simulated with MCS using 500 samples, and MCS both in Wishart matrix and parametric

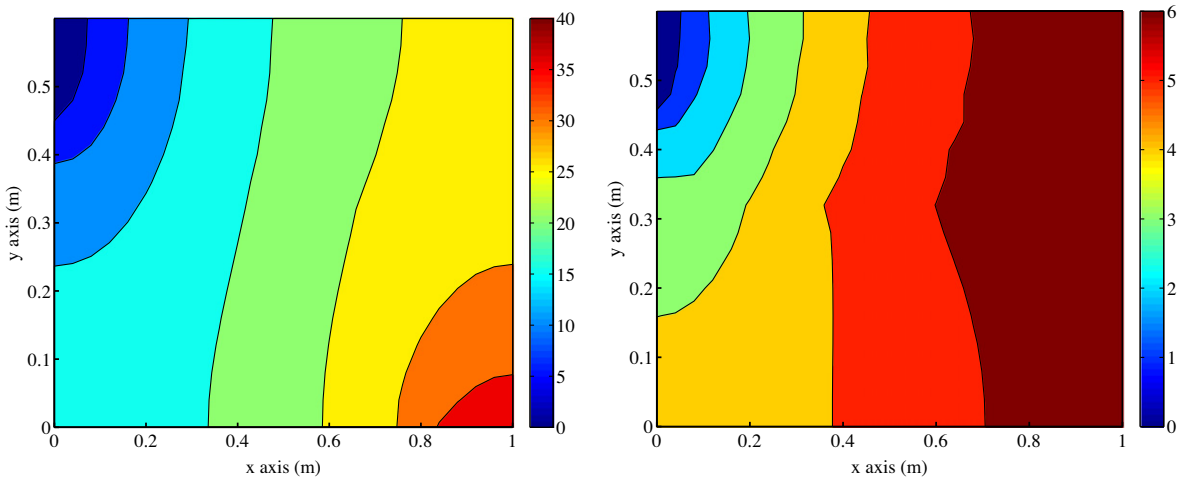


(a) Mean. (b) Standard deviation.

**Fig. 15.** Mean and standard deviation of the head obtained using the analytical expressions for parametric uncertainty with $\sigma = 0.1$ and Monte Carlo Simulation (MCS) for nonparametric uncertainty with $\delta = 0.05$, where positive definiteness of the global matrix is ensured through a sample selection procedure.

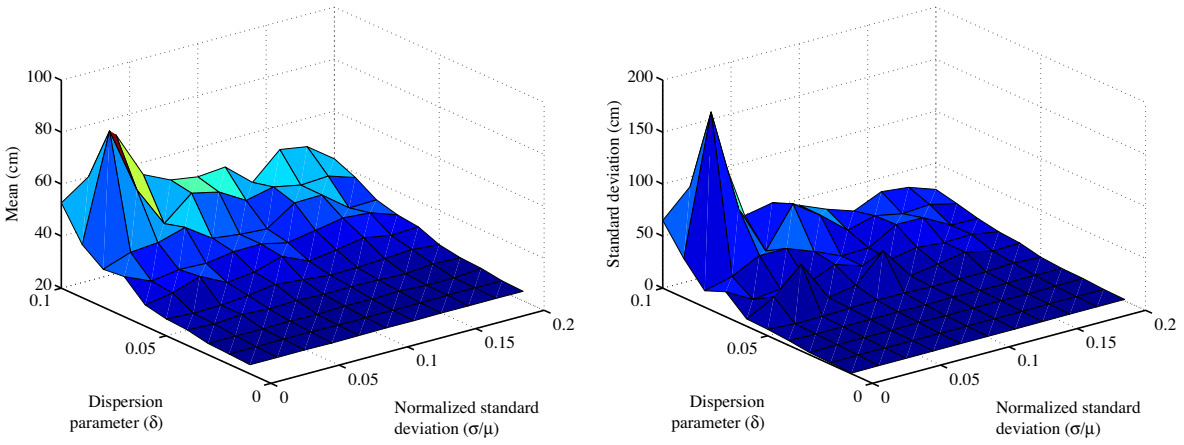


(a) Mean. (b) Standard deviation.

**Fig. 16.** Mean and standard deviation of the head at $(x,y) = (0.6923, 0.0400)$ obtained from the analytical expressions for parametric uncertainty and Monte Carlo Simulation (MCS) for nonparametric uncertainty, for different values of the dispersion parameter $\delta$ and the normalized standard deviation $\sigma/\mu$, where positive definiteness of the global matrix is ensured through a sample selection procedure.

uncertainty, using 500 samples for Wishart matrix results and 2000 samples for PC results within each Wishart sample.

In Fig. 19(a) it is observed that the mean increases with both $\delta$ and $\sigma/\mu$, while in Fig. 19(b) the standard deviation is almost constant in $\delta$ and increases linearly with $\sigma$. In Fig. 20(a) and (b) it is observed that the error in mean and standard deviation vary mostly with $\sigma/\mu$, as the dependance with nonparametric uncertainty has been calculated with MCS. The errors are small in comparison with the ones obtained for the beam problem. The error in mean is of the order of the one obtained from ensuring positive definiteness of the global matrix with sample selection, but the errors in standard deviation with this method doubles the ones obtained with the previous method.

## 6. Summary and conclusions

We consider stationary linear systems affected by two different types of uncertainties, namely, parametric uncertainty and nonparametric uncertainty in the context of finite element analysis. The first method deals with the case where both types of uncertainties cover the entire domain simultaneously. The parametric uncertainties are modelled by random fields and represented by their Karhunen–Loève (KL) expansions. The KL expansion of the system matrix in turn is used as the 'mean' matrix of the nonparametric model, which is represented by a Wishart random matrix model. The second combined method, considers both types of uncertainties appear over non-overlapping subdomains. The matrix representing the subdomain with nonparametric uncertainty is considered to be a Wishart random matrix and the matrix representing the subdomain with parametric uncertainty is represented by a KL expansion. The Wishart matrix model is obtained from a mean matrix and a dispersion parameter, quantifying the overall uncertainty. The random field model is characterized by its correlation length and standard deviation. The overall parametric and nonparametric uncertainties of the system are therefore quantified by the standard deviation of the the

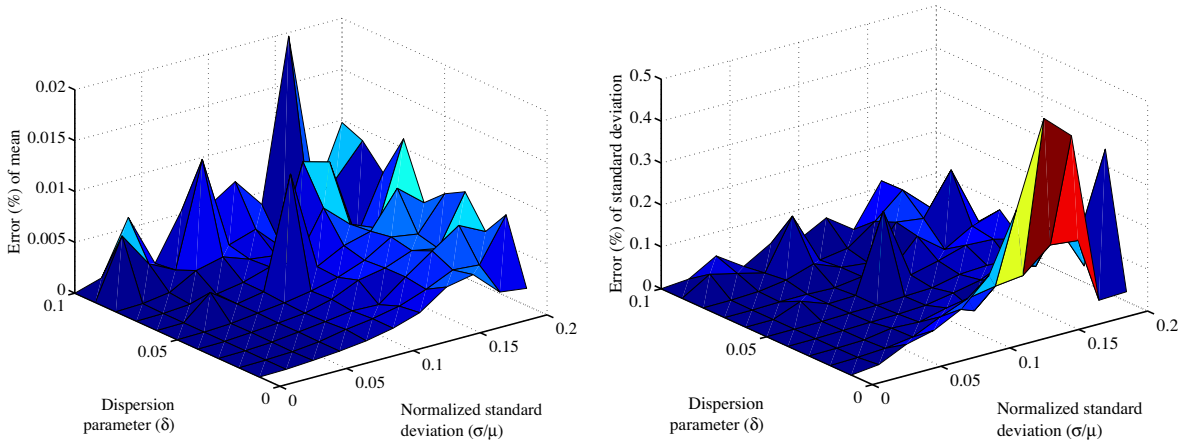


(a) Percentage error of mean. (b) Percentage error of standard deviation.

**Fig. 17.** Percentage error of mean and standard deviation of the head at $(x,y) = (0.6923, 0.0400)$ between the analytical expressions for parametric uncertainty and Monte Carlo Simulation (MCS), for different values of the dispersion parameter $\delta$ and the normalized standard deviation $\sigma/\mu$, where positive definiteness of the global matrix is ensured through a sample selection procedure.

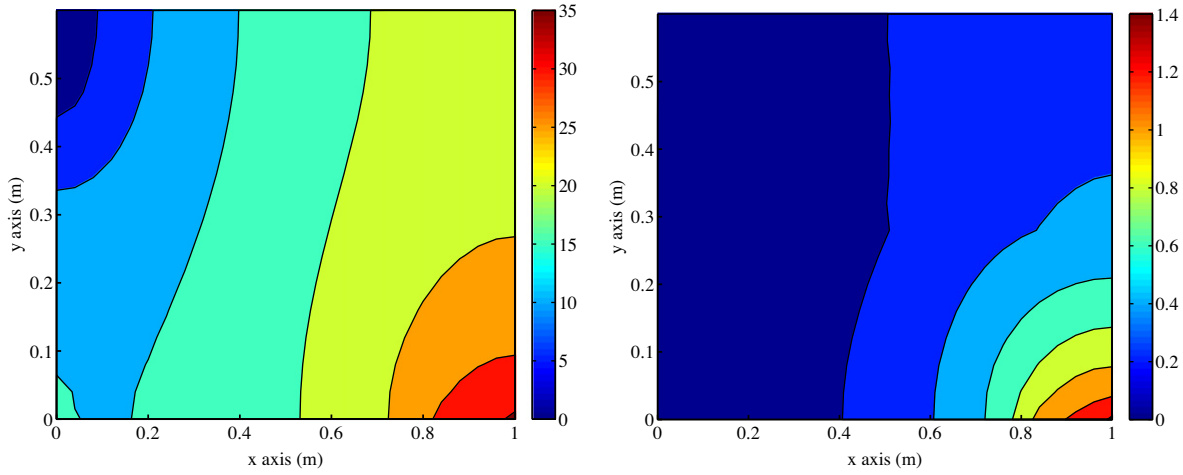


(a) Mean. (b) Standard deviation.

**Fig. 18.** Mean and standard deviation of the head, in cm, obtained using the analytical expressions for parametric uncertainty with $\sigma = 0.1$ and Monte Carlo Simulation (MCS) for nonparametric uncertainty with $\delta = 0.05$, where positive definiteness of the global matrix is ensured through a matrix correction procedure.

random field and the dispersion parameter of the Wishart random matrix model.

Two new approaches are developed for the propagation of the two proposed combined uncertainty model. Our approach exploits closed-form analytical results from the random matrix theory and Polynomial Chaos expansion method proposed for the stochastic finite element analysis. For the first kind of combined uncertainty, closed-form analytical expressions of the first two moments of the response are derived. For the second kind of uncertainty, expressions of the response are obtained using Polynomial Chaos expansion involving Wishart matrices. Two approaches, namely, matrix selection and matrix decomposition, are proposed to ensure the positive definiteness of the system matrix. Higher-order moments and probability density function of the response can be obtained by Monte Carlo simulation of the analytical expressions of the response derived in the paper.

Numerical examples on bending deformation of an Euler–Bernoulli beam and flow through a porous media are considered to illustrate the theoretical developments. Bending rigidity and hydraulic conductivity are considered to be random for these two problems respectively. Mean and standard deviations of the response are calculated for different values of dispersion parameters and standard deviations of the random field. Both of the proposed combined uncertainty modelling approaches are considered. Acceptable accuracies compared to direct Monte Carlo simulation results are observed. In summary, the contributions made in the paper include:

- Two new approaches to model combined parametric and nonparametric uncertainty in the context of probabilistic finite element method
- Novel analytical techniques based on unifying Polynomial Chaos expansion and random matrix theory results for the propagation of combined uncertainties

Future work is necessary to extend these techniques to dynamic problems and other types of differential equations such as hyperbolic and elliptic equations. Analytical work leading to establishing

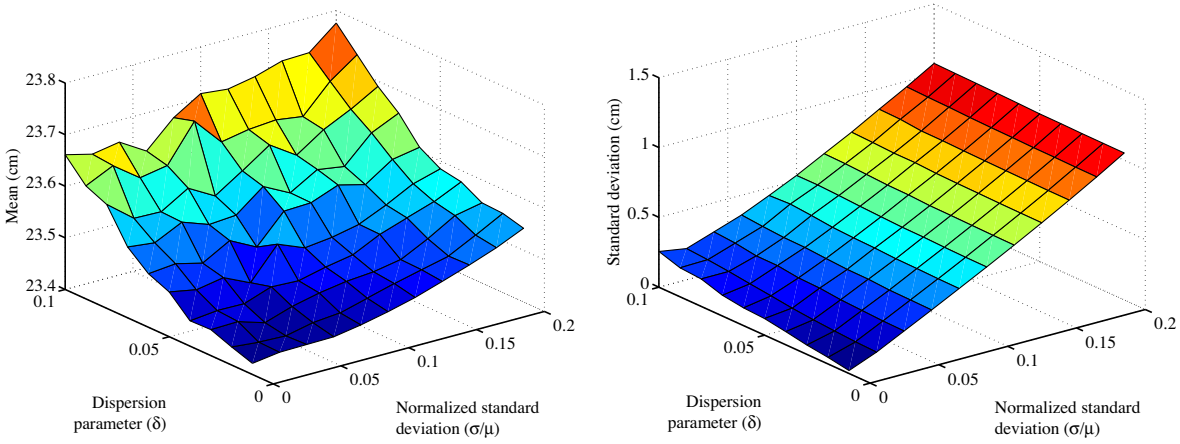


(a) Mean. (b) Standard deviation.

**Fig. 19.** Mean and standard deviation of the head at $(x,y) = (0.6923, 0.0400)$ obtained from the analytical expressions for parametric uncertainty and Monte Carlo Simulation (MCS) for nonparametric uncertainty, for different values of the dispersion parameter $\delta$ and the normalized standard deviation $\sigma/\mu$, where positive definiteness of the global matrix is ensured through a matrix correction procedure.

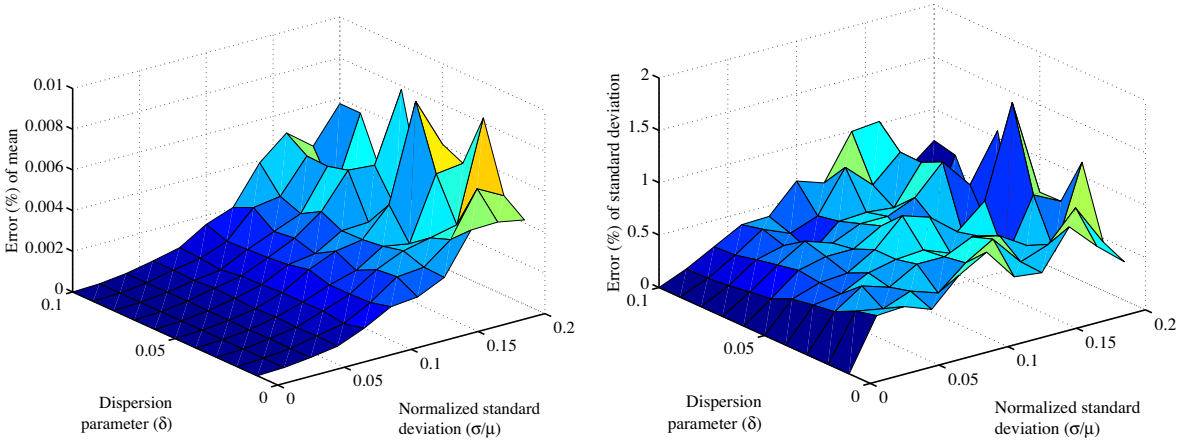


(a) Percentage error of mean. (b) Percentage error of standard deviation.

**Fig. 20.** Percentage error of mean and standard deviation of the head at $(x,y) = (0.6923, 0.0400)$ between the analytical expressions for parametric uncertainty and Monte Carlo Simulation (MCS), for different values of the dispersion parameter $\delta$ and the normalized standard deviation $\sigma/\mu$, where positive definiteness of the global matrix is ensured through a matrix correction procedure.

the positive-definiteness of the system matrices in a mathematically rigorous manner for the second case of combined uncertainty will also be a promising development.

## Acknowledgments

BP acknowledges the financial support from the Swansea University through the graduate research scholarship. SA acknowledges the financial support from The Royal Society of London through the Wolfson Research Merit Award.

## References

[1] Lin YK. Probabilistic thoery of strcutural dynamics. NY, USA: McGraw-Hill Inc; 1967.
[2] Zienkiewicz OC, Taylor RL. The finite element method. 4th ed. London: McGraw-Hill; 1991.
[3] Vanmarcke EH. Random fields. Cambridge Mass.: MIT press; 1983.
[4] Sudret B, Der-Kiureghian A. Stochastic finite element methods and reliability, Tech Rep UCB/SEMM-2000/08, Department of Civil & Environmental Engineering, University of California, Berkeley (November 2000).
[5] Stefanou G. The stochastic finite element method: past, present and future. Comput Meth Appl Mech Eng 2009;198(9-12):1031–51.
[6] Nouy A. Recent developments in spectral stochastic methods for the numerical solution of stochastic partial differential equations. Arch Comput Meth Eng 2009;16:251–85.
[7] Maître OPL, Knio OM. Spectral methods for uncertainty quantification: with applications to computational fluid dynamics. Berlin, Germany: Springer; 2010.
[8] Hurtado JE, Barbat AH. Monte carlo techniques in computational stochastic mechanics. Arch Comput Meth Eng 1998;5(1):3–29.
[9] Eldred MS, Burkardt J. Comparison of non-intrusive polynomial chaos and stochastic collocation methods for uncertainty quantification. In: 47th AIAA Aerospace Sciences Meeting including The New Horizons Forum and Aerospace Exposition, Orlando, Florida, Jan 5–8, 2009.
[10] Bressolette P, Fogli M, Chauvière C. A stochastic collocation method for large classes of mechanical problems with uncertain parameters. Probab Eng Mech 2010;25(2):255–70.
[11] Kleiber M, Hien TD. The stochastic finite element method. Chichester: John Wiley; 1992.
[12] Yamazaki F, Shinozuka M, Dasgupta G. Neumann expansion for stochastic finite element analysis. J Eng Mech, ASCE 1988;114(8):1335–54.

[13] Ghanem R, Spanos P. Stochastic finite elements: a spectral approach. New York, USA: Springer Verlag; 1991.
[14] Babuska I, Tempone R, Zouraris G. Galerkin finite element approximations of stochastic elliptic partial differential equations. SIAM J Numer Anal 2004;42(2):800–25.
[15] Nair PB, Keane AJ. Stochastic reduced basis methods. AIAA J 2002;40(8):1653–64.
[16] Matthies HG, Keese A. Galerkin methods for linear and nonlinear elliptic stochastic partial differential equations. Comput Meth Appl Mech Eng 2005;194(12-16):1295–331.
[17] Adhikari S. Stochastic finite element analysis using a reduced orthonormal vector basis. Comput Meth Appl Mech Eng 2011;200(21-22):1804–21.
[18] Chentouf S-A, Bouhaddi N, Laitem C. Robustness analysis by a probabilistic approach for propagation of uncertainties in a component mode synthesis context. Mech Syst Signal Process 2011;25(7):2426–43.
[19] Li CF, Feng YT, Owen DRJ. Explicit solution to the stochastic system of linear algebraic equations $(\alpha_1 A_1 + \alpha_2 A_2 + \cdots + \alpha_m A_m)x = b$. Comput Meth Appl Mech Eng 2006;195(44-47):6560–76.
[20] Falsone G, Ferro G. An exact solution for the static and dynamic analysis of Fe discretized uncertain structures. Comput Meth Appl Mech Eng 2007;196(21-24):2390–400.
[21] Gupta A, Nagar D. Matrix variate distributions. Monographs & surveys in pure & applied mathematics. London: Chapman & Hall CRC; 2000.
[22] Kapur JN. Maximum-entropy models in science and engineering. New Delhi: Wiley Eastern Limited; 1989.
[23] Gokhale DV. Maximum entropy characterizations of some distributions. Statistical distributions in scientific work 1975;3:299–304.
[24] Soize C. A nonparametric model of random uncertainties for reduced matrix models in structural dynamics. Probab Eng Mech 2000;15(3):277–94.
[25] Muirhead RJ. Aspects of multivariate statistical theory. New York, USA: John Wiely and Sons; 1982.
[26] Adhikari S. Wishart random matrices in probabilistic structural mechanics. ASCE J Eng Mech 2008;134(12):1029–44.
[27] Ghanem RG, Das S. Hybrid representations of coupled nonparametric and parametric models for dynamic systems. AIAA J 2009;47(4):1035–44.
[28] Matthies HG, Brenner CE, Bucher CG, Soares CG. Uncertainties in probabilistic numerical analysis of structures and solids - stochastic finite elements. Struct Safety 1997;19(3):283–336.
[29] Xiu DB, Karniadakis GE. The wiener-askey polynomial chaos for stochastic differential equations. SIAM J Scient Comput 2002;24(2):619–44.
[30] Le Maître OP, Knio OM, Najm HN, Ghanem RG. Uncertainty propagation using WienerHaar expansions. J Comput Phys 2004;197(1):28–57.
[31] Wan X, Karniadakis GE. An adaptive multi-element generalized polynomial chaos method for stochastic differential equations. J Comput Phys 2005;209:616–42.
[32] Wan XL, Karniadakis GE. Beyond wiener-askey expansions: handling arbitrary pdfs. J Scient Comput 2006;27(-3):455–64.
[33] Mohan PS, Nair PB, Keane AJ. Multi-element stochastic reduced basis methods. Comput Meth Appl Mech Eng 2008(197):1495–506.
[34] Chantrasmi T, Doostan A, Iaccarino G. Pad-legendre approximants for uncertainty analysis with discontinuous response surfaces. J Comput Phys 2009;228(19):7159–80.
[35] Gautschi W. On generating orthogonal polynomials. Soc Ind Appl Math 1982;3(3):345–83.
[36] Xiu D. Fast numerical methods for stochastic computations: a review. Commun Comput Phys 2009;5(2-4):242–72.
[37] Xiu D, Hesthaven JS. High-order collocation methods for differential equations with random inputs. SIAM J Scient Comput 2005;27(3):1118–39.
[38] Engels H. Numerical quadrature and cubature. London: Academic Press; 1980.
[39] Soize C. Maximum entropy approach for modeling random uncertainties in transient elastodynamics. J Acoust Soc Am 2001;109(5):1979–96. part 1.
[40] Adhikari S. Generalized wishart distribution for probabilistic structural dynamics. Comput Mech 2010;45(5):495–511.
[41] Soize C. Generalized probabilistic approach of uncertainties in computational dynamics using random matrices and polynomial chaos decompositions. Int J Numer Meth Eng 2010;81(8):939–70.
[42] Sampaio R, Cataldo E. Comparing two strategies to model uncertainties in structural dynamics. Shock Vib 2010;17(2):171–86.
[43] Sachdeva SK, Nair PB, Keane AJ. Hybridization of stochastic reduced basis methods with polynomial chaos expansions. Probab Eng Mech 2006;21(2):182–92.
[44] Maute K, Weickum G, Eldred M. A reduced-order stochastic finite element approach for design optimization under uncertainty. Struct Safety 2009;31(6). 450-450.
[45] Dawe D. Matrix and finite element displacement analysis of structures. Oxford, UK: Oxford University Press; 1984.
[46] Reddy JN. An introduction to the finite element models. Mc Graw Hill, Inc.; 1984.
[47] Smith BF, Bjorstad PE, Gropp WD. Domain decomposition: parallel multilevel methods for elliptic partial differential equations. Cambridge, UK: Cambridge University press; 1996.
[48] Sarkar A, Benabbou N, Ghanem R. Domain decomposition of stochastic PDEs: theoretical formulations. Int J Numer Meth Eng 2009;77(5):689–701.
[49] Ghosh D, Avery P, Farhat C. An FETI-preconditioned conjuerate gradient method for large-scale stochastic finite element problems. Int J Numer Meth Eng 2009;80(6-7, Sp. Iss. SI):914–31.
[50] Harville DA. Matrix algebra from a Statistician's perspective. New York: Springer Verlag; 1998.